18th AIAA/CEAS Aeroacoustics Conference (33rd AIAA Aeroacoustics Conference)
04 - 06 June 2012, Colorado Springs, CO
AIAA 2012-2209

Time-Domain Analysis of Excited Subsonic Jet Noise

M. Kearney-Fischer[1], A. Sinha[2] and M. Samimy[3]
Gas Dynamics and Turbulence Laboratory
Aeronautical and Astronautical Research Laboratories
Department of Mechanical and Aerospace Engineering, the Ohio State University
2300 West Case Road
Columbus, Ohio 43235-7531USA

Building on previous work showing that far-field jet noise has significant intermittent aspects and the statistical analysis of those intermittent aspects, the present work applies the same analysis techniques to an excited jet. Using an experimental database covering several operating conditions [jet Mach number (M_j = 0.9), nozzle diameter (D = 2.54 cm), and jet stagnation temperature ratios (TTR = 1.0 – 2.5)] and a wide array of excitation parameters (m = 0, 1, & 3 and St_{DF} = 0.09 – 3.0), these events are extracted from the far-field noise signals measured in an anechoic chamber. This database is analyzed to determine what characteristics of these noise events and their production can be identified with the aid of excitation. Understanding of the impact of the excitation is leveraged to inform discussion of the statistical results and their relationship to the jet flow dynamics. Analysis of the excited jet reveals the existence of a resonance condition. When excited at the resonance condition (discussed in terms of a relationship between the noise event mean intermittence and the spectral peak frequency at shallow angles), large noise amplification can occur – this is associated with each large-scale structure producing a noise event. Conversely, noise reduction occurs when only one noise event occurs per several large-scale structures. The results indicate that there seems to be a competition for flow energy among neighboring structures that dictates if and how their dynamics will produce noise that radiates to the far-field. The interaction of large-scale structures is explored and these results are related to the acoustic results.

1 INTRODUCTION

Six decades of research have not yet revealed a clear understanding of jet noise [1, 2]. While there have been advances in empirically based models [e.g. 3, 4] and theoretical analysis [e.g. 5] of jet noise, the essential features of jet noise are still debated. Without a complete description of the essential features of jet noise, understanding of their sources is clearly impeded.

There have been two dominant methods of experimental data analysis in jet aeroacoustics: 1) Fourier spectrum analysis and 2) correlation analysis. Spectral analysis is the fundamental tool used by the aeroacoustics community, and for good reason. These two tools provide researchers with a wealth of information and insight, but with certain restrictions. Spectral analysis discards temporal information making it impossible to link particular aspects of the frequency domain back to segments of the signal in time. Correlation analysis provides links between two signals in time, but only if their trends are sufficiently similar – it can indicate how similar the trends of two signals are and how the similarity is displaced in time.

These two tools are likely overlooking some of the fundamental aspects of jet noise. Recently, wavelet transforms are starting to be used to obtain a more complete picture of the noise signal. The basic theme of these works is the supposition that acoustically subsonic jet noise (at least in the radiation to aft angles) is made up of intermittent bursts as opposed to continuous variations. If this assertion is presumed to be accurate, understanding this kind of signal requires a different analysis methodology than has been prevalent in the literature. In a recent work from the Gas Dynamics and Turbulence Laboratory (GDTL) of the Ohio State University, Kearney-Fischer *et al.* [6] used a peak identification technique to isolate intermittent bursts (in this context defined as portions of the signal that exceeded 1.5 times the root mean square far-field pressure fluctuations, 1.5 p_{RMS}) in the noise signals

[1] Currently Sr. Aeronautical Engineer at Lockheed Martin Aeronautics, AIAA Member
[2] Currently postdoctoral researcher at Caltech, AIAA Member
[3] The John B. Nordholt Professor, AIAA Fellow, Corresponding author: samimy.1@osu.edu

from a wide range of polar angles and jet operating conditions. This previous study showed that these bursts (hereafter referred to as noise "events") are the dominant feature of the noise signals at low polar angles relative to the jet downstream axis. Additionally, an in depth statistical analysis of these events was conducted revealing trends relevant to the understanding of jet noise (e.g. noise events are statistically independent phenomena, noise event characteristics in unheated jets scale with diameter and not jet acoustic Mach number). The purpose of the present work is to take this previously developed analysis methodology and understanding and apply it to an excited jet to see how the statistical quantities are altered when the instability dynamics of the jet are controlled.

2 BACKGROUND

It is generally accepted that jet noise is produced by the interaction and development, as well as the disintegration of turbulent structures. Beyond this point, the description of noise production processes gets quite complicated. In subsonic jets, the evolution, interaction, and disintegration of flow structures produce what is known as mixing noise. Theoretical approaches to the problem have provided insights, but an elegant description of a source and its relationship to the noise produced has not been obtained. Theoretical analyses, beginning with the pioneering work of Lighthill, struggle to untangle the non-linear nature of the governing equations into a form that clearly identifies a source.

2.1 Vortex Sound

It has been speculated that dynamically significant events, as opposed to the mere existence of the structures, (e.g. the collision/interaction of two vortices or breakup of a vortex) are the mechanism that produces the noise radiated to the low angles. The experimental work of Kambe *et al.* [7-9] shows that vortex sound theory [e.g. 10, 11] does a reasonably good job of predicting the noise generated by the head-on collision of two vortex rings. The sound pressure signal p produced by these collisions appears as a primary peak accompanied by two lower amplitude side-lobes. Their work has also shown that these collisions produce a primarily quadrupole sound field whose amplitude scales as $p \propto U^4/r$ where U is the collision speed of the vortices and r is the radial distance to the observation point. In terms of intensity, these collision noise events follow the same U^8 scaling as derived by Lighthill for jet noise. Additionally, they revealed that these events have a non-dimensional characteristic lifetime that scales as R_o/U, where R_o is the initial radius of the vortex rings.

Another important example of experimental work on vortex sound is the research of Schram *et al.* [12, 13]. This work focuses on the sound generated by ring vortex pairing events in low-speed jets ($U_j \approx 5$ & 34 m/s). Using a combination of excitation, axisymmetric geometry assumptions, and PIV, they were able to calculate the integrated source term from the velocity field and, therefore, calculate the acoustic pressure fluctuation produced by the pairing. By examining two different jet velocities, they observed that the structure of the acoustic pulse became more complex with increasing velocity. In the 5 m/s jet, vortex pairing produced an acoustic pulse that was essentially a single prominent peak with weak side-lobes of opposite sign. In the 34 m/s jet, pairing resulted in an acoustic pulse with two prominent peaks, one positive and one negative, with an additional weaker lobe on each side of the primary pulse.

Although much of the experimental work has focused solely on the head-on collision of two vortex rings, the sound produced by this well-studied type of vortex collision is a reasonable model for the kinds of sound events created by various unsteady vortex processes. There have also been theoretical and simulation-based works looking at a wider variety of vortex phenomena and their sound production [e.g. 14-17]. This is an ongoing and active area of research and its precise relevance to jet noise is still unclear.

2.2 Flow Control

Experiments on controlling the development of the jet plume have been going on for almost as long as jets have been in use. Previous studies of jet flow control include both passive (geometrical modifications of the nozzle such as chevrons, lobed nozzles, etc.) [e.g. 18-23] and active (can be turned off to eliminate performance penalties when unneeded) control techniques [e.g. 24-30].

Jets have several instabilities which have been well researched in low-speed and low Reynolds number jets [e.g. 24-34]. These instabilities are: the jet initial shear layer instability, the jet column or jet preferred mode

instability, instability related to significant density gradients in the jet, and, in the case of an axisymmetric jet, the azimuthal component of instability.

In experimental work simulating practical conditions, as the Reynolds number of the jet increases for a given jet diameter and dynamic viscosity, so does the background noise, the instability frequencies, and the flow momentum. To operate in this environment, active control devices (actuators) must provide excitation signals of increasingly large amplitude and frequency. As a result, the limited works in the active control of high-speed and high Reynolds number jets used acoustic excitation to control high subsonic jets around their preferred mode [35-37]. There have been a few experiments which used active control in supersonic jets [e.g. 37-42]. Unfortunately, acoustic drivers lose control authority in these highly energetic jets at Reynolds numbers (typically control authority wanes for Reynolds numbers greater than 100,000) which are too low to explore the dynamics of high speed and high Reynolds number jets used most commonly in application (i.e. jet engines). The loss of control authority occurs because a more energetic flow requires a greater input of energy to perturb the flow. Consequently, a new type of actuator is required, which can operate in this environment. For additional information on flow control mechanisms, see the following previous works from GDTL [43-46].

GDTL has developed a class of plasma actuators, called localized arc filament plasma actuators (LAFPAs) that can provide excitation signals of high amplitude and high frequency for high-speed and high Reynolds number flow control [47, 48]. These actuators work by exciting the instabilities that exist in the jet. GDTL has used these actuators for noise and flow control studies in both subsonic and supersonic unheated jets [e.g. 43-46, 49]. More recently, GDTL started exploring the impact of jet temperature on the effectiveness of LAFPAs. The effect of heating on LAFPA performance for both mixing enhancement and noise mitigation is currently under investigation in both subsonic and supersonic jets [e.g. 50-53].

It should be noted that the structures in jets excited by this active control method have a primarily span-wise extent – in this context, span-wise means that the vortex axis is aligned with the azimuthal axis of the jet. Previous works [45] have shown that excitation with these actuators produces regular structures over a wide range of frequencies and that the induced structure spacing is dictated by the excitation frequency. While not discussed here in detail, various data reduction methods such as the jet width, turbulent kinetic energy, phase locking, proper orthogonal decomposition, and vortex identification techniques have been used to characterize the behavior of the excited large-scale structures. Based on these analyses, several conclusions were reached about the excited large-scale structure characteristics.

1. The largest structures are created by exciting the jet near the jet column natural Strouhal number ($St_{DF} \approx 0.3$). The subscript "F" denotes an excitation frequency.
2. The largest structures are created by exciting mode ±1, mode 1, and then mode 0 in decreasing order of size.
3. Individual structures created by excitation are detectable from $St_{DF} \approx 0.1$ (the lowest Strouhal number ever examined) to $St_{DF} \approx 1.5$. Each firing of an actuator within this frequency range generates a structure.
4. Depending on the azimuthal mode of the excitation, the structures created by the individual actuators merge into different shapes (e.g. mode 0 merges into a ring, mode 1 into a helix, etc.). The rate at which this merger occurs depends on the forcing azimuthal mode and also the excitation frequency.
5. Structures excited near $St_{DF} \approx 0.7$ initially grow more rapidly than those at $St_{DF} \approx 0.3$ and then convect for a few jet diameters (about 2-4) without significant development. This is particularly true of mode 0 and this behavior is accentuated at elevated temperatures.

2.3 Temporally Localized Signal Analysis

Fourier analysis utilizes oscillating signals with infinite extent and describes the examined signal in terms of those oscillations. Therefore it is not particularly useful for characterizing localized events. There is some precedent in the literature for jet noise analysis assuming a fundamentally intermittent signals [e.g. 54-62]. A common theme that unifies these works is the use of wavelet analysis – the underlying principle of which is that the signals under examination cannot be adequately described by a set of periodic waves. This assumption of intermittence has produced some interesting results.

In the case of the previous works at GDTL [54, 55], the assumption of intermittence provides a basis for a source localization method. A wavelet transform of the far-field signal showed that there were spikes in the signal. Based on this observation, noise events were defined as spikes rising above a specified threshold in the time domain. The localization method used a microphone array, and the times of arrival at the various microphones of these spikes to locate the source of an event in space-time. As discussed in those works, the calculated region of noise sources agrees with other research indicating that the noise radiated at low angles (~30°) relative to the jet downstream axis comes from an area near the end of the potential core. Simultaneous flow-visualizations using a MHz-rate imaging

system showed that these events are associated with dynamically significant behavior of the large-scale structures. Guj *et al.* [60] used a similar kind of conditional averaging of the flow-field to determine that bursts of noise were related to dynamically significant fluctuations of the large-scale structures. They also called attention to the limitations of Fourier analysis to illuminate this kind of phenomenon.

Cavalieri *et al.* [57] looked at the direct numerical simulations (DNS) of an uncontrolled and an optimally noise-controlled two-dimensional mixing layer of Wei and Freund [63]. They showed that the optimally controlled case accomplishes noise reduction by suppressing certain intermittent peaks in the signal – highlighting the need to include intermittency in sound prediction schemes. Noise suppression in this simulation was related to preventing the merger of three vortices (a triple-merger) that was shown to produce a large spike in the acoustic signal. Cavalieri *et al.* [58] discuss a wave-packet model in which the envelope function varies in both space and time. This analysis, which follows the idea originally suggested by Kastner *et al.* [64], shows that a high amplitude event (i.e. a pressure spike) can be produced when the wave-packet is truncated by fluctuations in the envelope. Grassucci *et al.* [56] used a wavelet domain filter to separate near-field pressure fluctuations into intermittent and non-intermittent signals. They then related the intermittent signal to velocity fluctuations in the jet using Linear Stochastic Estimation (LSE). While this work is preliminary, their initial results are promising. Kœnig *et al.* [59, 65, 66] have started using wavelet transforms and filtering in the wavelet domain to isolate these intermittent events for study. This analysis uses a 4^{th} order Paul wavelet to decompose the signals with a continuous wavelet transform. Results to date have mainly focused on the relationship of the resulting directivity patterns to wave packet models for jet noise. One important observation in Kœnig *et al.* [65] is that using Helmholtz number can achieve better spectral collapse for varying acoustic Mach number than Strouhal number scaling in unheated jets. This scaling with Helmholtz number has also been seen by other researchers [e.g. 67]. Low *et al.* [62] uses wavelet filtering and correlation on both near and far-field to determine how the near-field events are related to the far-field events. Their work is still preliminary, but warrants mentioning as a significant attempt to trace the intermittent aspects of jet noise back toward their sources.

These works show that jet noise does indeed contain intermittent events and that these events play a significant role in the overall acoustic picture of the jet. The results to date, however, are quite limited in their description of these intermittent events. Issues such as the importance of these events to the total signal spectra, many aspects of the nature of these events (lifetimes, frequency of occurrence, etc.), and exact relationship of these events to the flow-field dynamics remain to be determined.

2.4 Noise Event Definition and Identification Method

The two essential features of the noise event definition used in this work are: 1) primary noise sources in a mixing noise dominated jet (i.e. acoustically subsonic), at least those that radiate to shallow angles relative to the jet downstream axis, are intermittent "events" with periods of relative silence in between; and 2) a noise event is defined as a contiguous set of points whose peak amplitude exceeds $\pm 1.5 p_{RMS}$. The validity of this noise event definition has been established on a large dataset in a previous work from GDTL [6]. A detailed description of the noise event extraction method is given in [6] so only a concise description is provided here. It should be noted that the exact same analysis algorithm used in the previous work is applied to the data in the present work. None of the parameters of the algorithm were adjusted in any way. For any identified event, its amplitude (A_i), width (δt_i – defined as the full width at half maximum), and location in time (T_i) are extracted. For the exclusive purpose of calculating the spectrum of a signal containing only these events, each event is reconstructed using the three parameters just mentioned and a Mexican hat function. Events are assumed to be independent and so the reconstructed signal is a superposition of the individual events. It should be noted that event location and width are determined to single sample accuracy of the discretely sampled acoustic signal and are not interpolated to a higher precision. One consequence of this data extraction method is that the minimum event width allowed is three samples. Any subsequent analysis of these quantities will also be quantized at single sample accuracy.

3 EXPERIMENTAL SETUP

All of the experiments on excited jets are conducted in the anechoic chamber at GDTL within the Aeronautical and Astronautical Research Laboratories (AARL) at Ohio State University.

3.1 Test Facility

The jet simulation facility at GDTL is of blow-down type. The compressed air, supplied with three 5-stage reciprocating compressors, is filtered, dried, and stored in two cylindrical tanks with a volume of 43 m^3 and pressure up to 16 MPa. The compressed air is passed through a storage heater at a set temperature to heat up the air to the desired temperature and supplied to the stagnation chamber of the jet facility with an axisymmetric nozzle. The air is discharged horizontally through the nozzle into an anechoic chamber and then through an exhaust system to the outdoors (Fig. 1). The anechoic chamber in these experiments has an open volume of about 25 m^3 and is rendered anechoic down to about 250 Hz using fiberglass wedges. The chamber validation is documented in Kerechanin *et al.* [68]. The nozzle for the experiments reported in this work is stainless steel, axisymmetric with an exit diameter of D = 2.54 cm (1 in.).

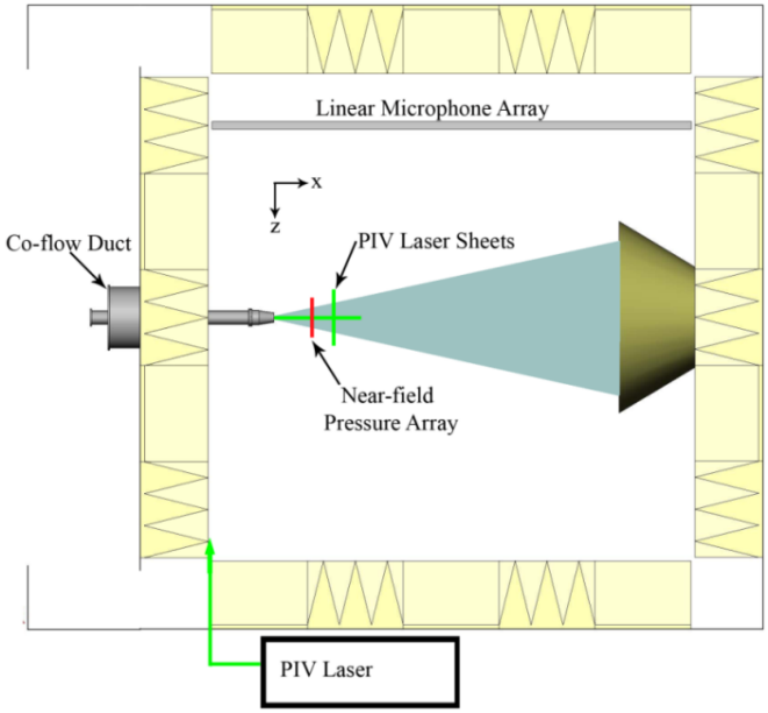

Fig. 1: Jet facility and anechoic chamber.

3.2 Plasma Actuators

As discussed in §2.2, GDTL has developed a type of flow control actuator known as the Localized Arc Filament Plasma Actuator (LAFPA). Each actuator consists of a pair of pin electrodes held in place using a nozzle extension. The electrodes are distributed around the nozzle perimeter, approximately 1 mm upstream of the nozzle extension exit plane. The nozzle extension is made of boron nitride and tungsten wires of 1 mm diameter are used for electrodes. Measured center-to-center, the spacing between a pair of electrodes for each actuator is 4 mm, and the distance between the neighboring electrodes of two adjacent actuators is 6 mm. With this arrangement, eight actuators are uniformly distributed around the nozzle extension so that the azimuthal spacing between two adjacent actuators is 45º. More information on the plasma actuators can be found in previous publications from GDTL [e.g. 47, 48].

3.3 Acoustic Measurements

The primary diagnostic tool used in the work discussed here is a far-field acoustic system. The far-field sound pressure level (SPL) is measured using ¼ inch Bruel & Kjaer 4939 microphones. Acoustic data are collected using a linear microphone array with ten microphones measuring angles of ϕ = 25°, 30°, 35°, 40°, 45°, 50°, 60°, 70°, 80°, and 90° relative to the jet downstream axis. The array axis is parallel to the jet axis and the microphones are mounted normal to the array axis. Testing confirmed that the only observable changes in spectra acquired with the

microphones mounted as described, as opposed to radial (also referred to as normal) incidence, are due to the sensitivity of the microphones. The resulting radial distances from the nozzle exit to the microphones range from 49*D* (at 90°) to 116*D* (at 25°). The acoustic signal from each microphone is band-pass filtered from 20 Hz to 100 kHz, amplified by one of three four-channel Bruel & Kjaer Nexus 2690 conditioning amplifiers, and acquired using National Instruments PXI-6133 A/D boards and LabView software. The microphones are calibrated using a 114 dB, 1 kHz sine wave, and the frequency response of the microphones is flat up to 80 kHz with the microphone grid cover removed. Sample signals are collected at 200 kHz with 8192 data points per segment producing a spectral resolution of 24.4 Hz. An average sound pressure level (SPL) spectrum is obtained from the mean square of 100 short-time spectra. More information on the microphone hardware and spectral analysis techniques is available in [52].

3.4 Experimental Parameters

Since the goal of this work is to explore mixing noise from subsonic jets, a jet with a hydrodynamic Mach number of 0.9 at different Total Temperature Ratios (TTR) was chosen for study. Some quantities relevant to the experimental operating conditions—the Reynolds number (Re_D), acoustic Mach number (M_a), and Exit Temperature Ratio (ETR)—are computed in Table 1. While some of these cases aren't acoustically subsonic in the strictest sense ($M_a < 1$), a previous work has shown that these jets do not display any strong supersonic noise characteristics [69]. Based on that result, it was determined that the data from these experiments was acceptable for the analysis undertaken in the present work.

D (cm)	M_j	TTR	$Re_D \times 10^{-5}$	M_a	ETR
2.54	0.9	1.0	6.12	0.83	0.86
		1.5	3.65	1.02	1.29
		2.0	2.57	1.18	1.72
		2.5	1.98	1.32	2.15

Table 1: Experimental operating conditions.

The excitation parameters used on these jets are shown in Table 2 – the subscript "*F*" signifies forced and is used to denote an excitation quantity for several variables. Previous works [e.g. 52] showed that the changes in the acoustic field of the jet were minimal outside this frequency range. The axisymmetric mode ($m = 0$) and the 1st order helical mode ($m = 1$) are canonical choices for excitation based on the literature discussed in §2.2. Additionally, Suzuki and Colonius [70] have shown that azimuthal $m = 0$ mode growth in an unexcited jet is significantly more enhanced by heating of the jet than that of modes 1 and 2. This same phenomenon has also been reported by Hall and Glauser [71] and previous work by GDTL [53] discusses some experimental results of this behavior with respect to LAFPAs. Previous work showed that $m = 3$ (the highest mode accessible by the 8 actuators used) produced the greatest reductions in the far-field noise levels [e.g. 52]. The excitation parameter space (Table 2) is based on these observations. A spectral analysis of this data has been published in a previous work [52] and additional discussion of the data can be found there.

Azimuthal Mode (m)	0, 1, 3
Excitation Strouhal Number (St_{DF})	0.09 – 3.0

Table 2: Excitation parameters.

4 EXCITED JET ANALYSIS

In this section, the impact of excitation on the noise events is analyzed using the GDTL database. This is accomplished by first performing a spectral analysis of the data to determine how the jet responds to excitation using the traditional tool. The reason for this is to identify excitation cases that produce the greatest changes in the Sound Pressure Level (SPL) and/or the Overall Sound Pressure Level (OASPL) and then to relate those changes to changes in the noise event characteristics.

4.1 Spectral Analysis

In the previous works from GDTL on the acoustic field of an excited jet, it has been common to remove narrowband tones associated with excitation to focus on the changes in the broadband spectral shape [e.g. 52, 72]. This was done for two reasons: 1) there is potentially a component of the signal acquired by the DAQ system that is electronic noise associated with the plasma based excitation, and 2) the actuators emit a compression wave that is detectable at the microphones (referred to as actuator self-noise). It has been determined in previous works that these contaminants were relatively weak, but it will always be difficult to tell what portions of the narrowband tones originate in the flow-field. Given the obvious complications associated with attempting to extract the time domain signature of the electronic noise and compression waves associated with excitation without impacting the noise produced by the jet, it will be assumed that the signal as acquired is valid and no attempt to condition the data will be made.

The experimental data used in this analysis is well documented in a previous GDTL publication [52] so only selected aspects of the spectral analysis are discussed in this paper.

4.1.1 Changes in OASPL

The changes in OASPL for the angular domain as a function of excitation Strouhal number are presented and discussed to determine how the excitation parameters impact the noise. The ΔOASPL (in dB) maps ($OASPL_{FORCED} - OASPL_{BASELINE}$) for mode 0 at various temperatures are shown in Fig. 2 and sample maps for modes 1 and 3 are shown in Fig. 3. The discussion of these results will focus on one temperature at a time.

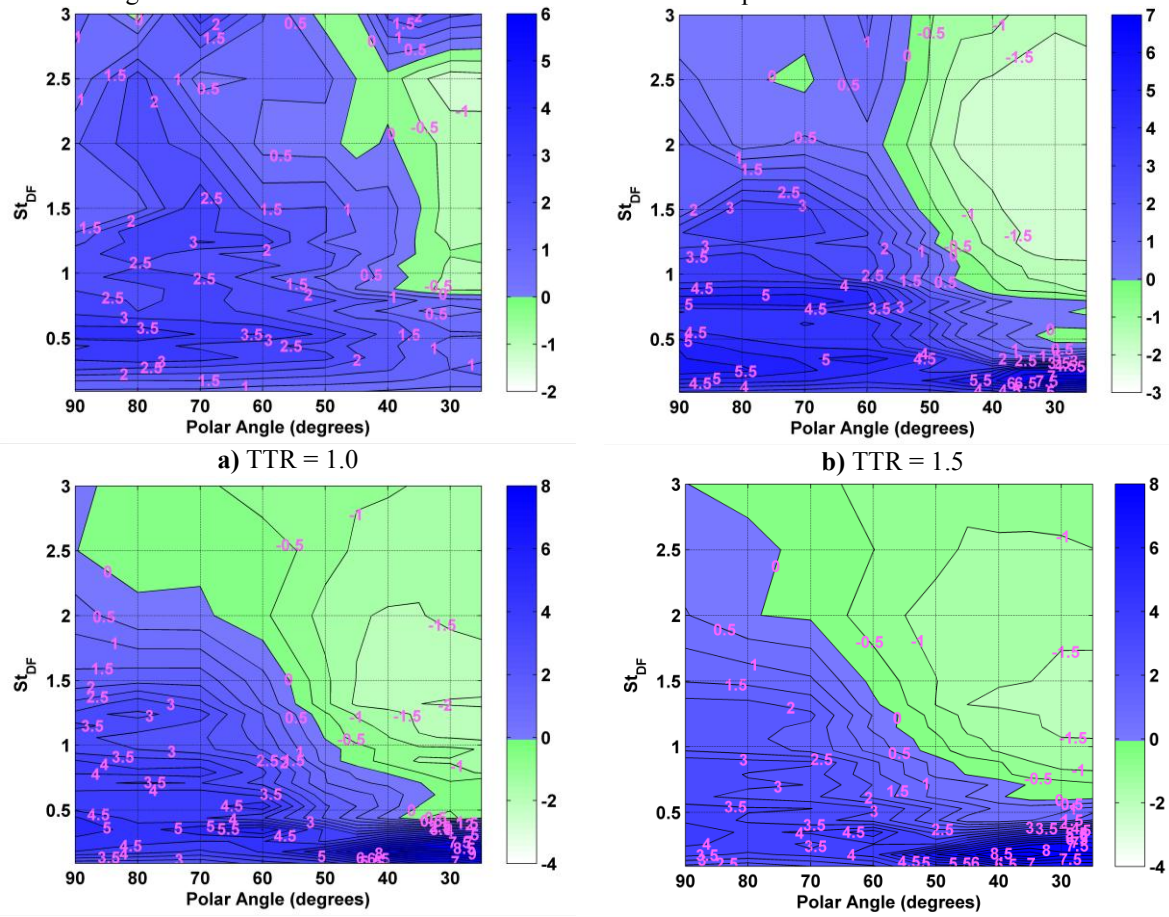

a) TTR = 1.0 **b)** TTR = 1.5

c) TTR = 2.0 **d)** TTR = 2.5

Fig. 2: ΔOASPL (dB) for $m = 0$ – reproduced from [52].

In the unheated cases, there is some consistency in the reductions observed at the small angles and the general amplification over most of the angles and excitation Strouhal numbers, but the generally erratic behavior indicates

that the energy of the narrowband tones is playing a significant role in the measured OASPL. Furthermore, the variation in the energy of the narrowband tones as a function of the excitation frequency makes it difficult to discern any trends in the data. The narrowband spectra show (see [52] for detailed discussion and figures) that the broadband jet noise is being altered, but the complex nature of these ΔOASPL maps makes interpretation almost impossible.

The results at the elevated temperatures show that the data become much more organized as the temperature increases. In mode 0, there is a strong amplification region at the low excitation frequencies and low angles. In contrast, modes 1 and 3 have no such strong amplification region. These results clearly show that by proper selection of St_{DF} and excitation azimuthal mode, one can obtain noise reduction across all measured radiation angles for temperature ratios $\geq$ 2.0. A more detailed examination of the ΔOASPL maps yields the following observations, but most of the conclusions are withheld until the time-domain statistics have been analyzed (§4.2).

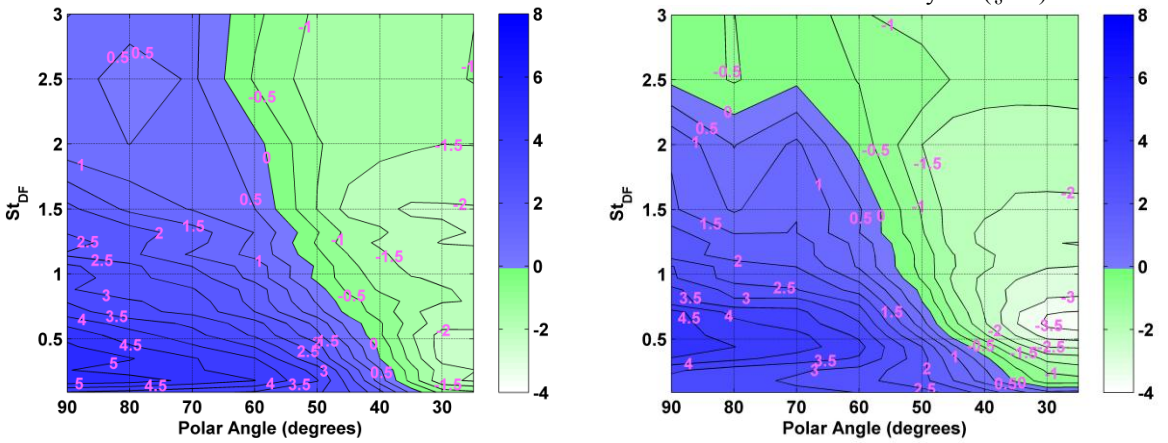

a) $m = 1$ **b)** $m = 3$

Fig. 3: Sample ΔOASPL (dB) for other azimuthal modes at TTR = 2.0 – reproduced from [52].

1. The far-field noise signature of the unheated jet seems to contain a significant amount of actuator self-noise that obscures trends in the OASPL. This diminishes as the jet is heated because the jet gets louder.
2. In the elevated temperatures, m = 0 develops a strong increase in OASPL at the low angles (ϕ < 50°) for excitation Strouhal numbers near jet column natural frequency ($St_D \approx 0.3$). Close inspection reveals that the greatest increase occurs at the excitation frequency of St_{DF} = 0.18 – near the spectral peak frequency. This suggests, based on the unexcited results [6] that link the mean intermittence ($\overline{\Delta T}$) to the spectral peak frequency, that exciting the jet with mode 0 at that frequency reinforces the naturally occurring events. Examination of the narrowband spectra indicates that this additional energy is contained in the narrowband tones. Since this behavior is not observed in the other modes, it is concluded that this is a flow-field response as opposed to actuator electronic noise or self-noise. The cause for this is likely the confluence of two separate mechanisms: a disproportionate increase in m = 0 energy content in unexcited heated jets and superdirective radiation. The latter will be discussed more in subsequent sections.
3. While difficult to determine from the lower temperatures alone, the complete picture indicates that m = 3 produces the largest decreases in the OASPL and that these decreases occur at the lowest angles measured (ϕ = 25° & 30°).
4. The excitation Strouhal number that removes the most energy at the low angles decreases with increasing temperature and is different for the different azimuthal modes. Mode 0 settles near $St_{DF} \approx 1.3$, while modes 1 and 3 settle at $St_{DF} \approx 0.5$.
5. Reduction at the low angles is generally accompanied by amplification at the higher angles.

It has been observed that the amount of energy found in the m = 0 flow-field mode of unexcited jets grows disproportionately faster than the other modes with increasing jet temperature [70, 71]. Reinforcing this natural mechanism with excitation would likely produce axisymmetric flow-field structures that have significantly increased spatial and temporal coherence – a conclusion that is supported by a previous work using PIV [53]. Another way to say this would be that the flow becomes more receptive to m = 0 development. The concept of superdirective radiation in jet noise, originally discussed by Crighton and Huerre [73], describes the radiation pattern from a noise source that can't be decomposed into a finite series of multipoles. In an unexcited jet, there are a wide range of oscillation frequencies with randomized phases that would result in energy being distributed in time and frequency

space. If one frequency becomes dominant (say through the combination of disproportionate increases in mode receptivity and excitation), the energy of the radiation should be concentrated in both time and frequency space. The directive aspects of the ΔOASPL map and the narrowband spectra support this assertion. The observation of this phenomenon only in the axisymmetric mode suggests that the spatial coherence of the structures (and consequently the wave-packets) is an important factor in the radiating efficiency of this mechanism.

To facilitate discussion in subsequent sections, the ΔOASPL plots for $\phi = 30°$ are shown in Fig. 4.

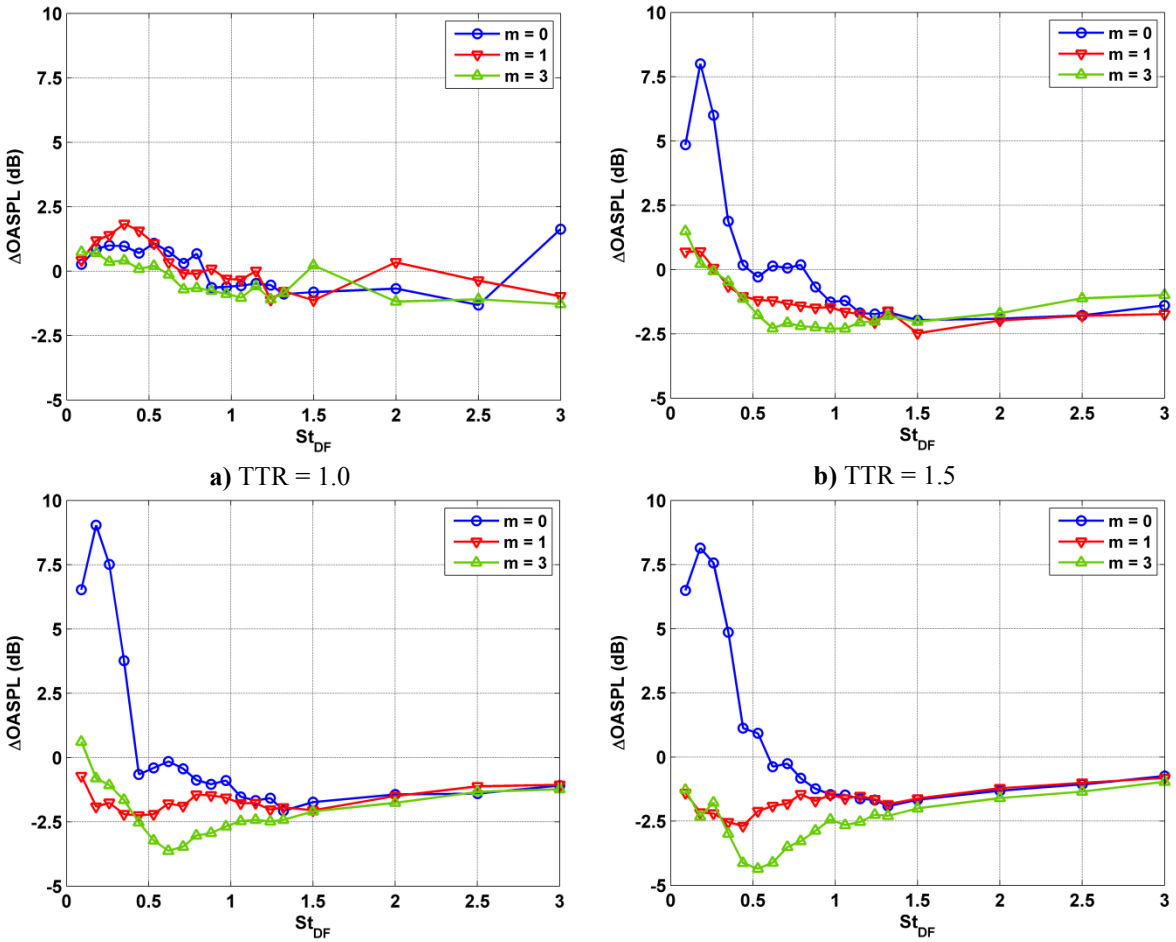

a) TTR = 1.0 **b)** TTR = 1.5

c) TTR = 2.0 **d)** TTR = 2.5

Fig. 4: ΔOASPL plots for $\phi = 30°$.

4.1.2 Events-Only Comparison

Using the same process described for the unexcited jet data analyzed in [6], the spectra of the events-only signal are constructed and plotted in Fig. 5 for unexcited cases as well as two representative sets of excitation parameters at two of the four temperature ratios. The unexcited results are very similar to the results in [6], which confirms the generality of the results as well as the procedure, so they are not discussed in detail.

The spectral behaviors in the excited jet are qualitatively similar to the unexcited jet results [6] in most cases and the spectral reconstruction characteristics for temperatures and excitation parameters not shown are also qualitatively similar to those presented. For the unheated jet, the reconstruction of the low-angle data is quite good and the sideline angle data has some problems. At high frequencies, the sideline spectra are highly distorted and elevated (taking on an almost completely flat profile—white noise). The reasons for this reconstruction deficiency at the sideline angles have already been discussed [6]. In the elevated temperatures, the sideline spectra results are similar to the cold jet, but something more complicated is happening with the low angles. For the case shown in Fig. 5d, the 30° spectral peak location is reasonably good, but the spectral amplitude is significantly over-predicted. Additional spectra for the same operating condition and excitation frequency are shown in Fig. 6. These additional

spectra show that this behavior is only present in the axisymmetric mode. Examining spectra at nearby frequencies and polar angles (not shown) reveals that this behavior occurs in the region of the ΔOASPL maps where strong amplification was observed. This over-prediction is another indicator that something different is happening in the acoustic field when the jet is excited axisymmetrically near the jet column natural frequency (St_D = 0.3) in these heated cases.

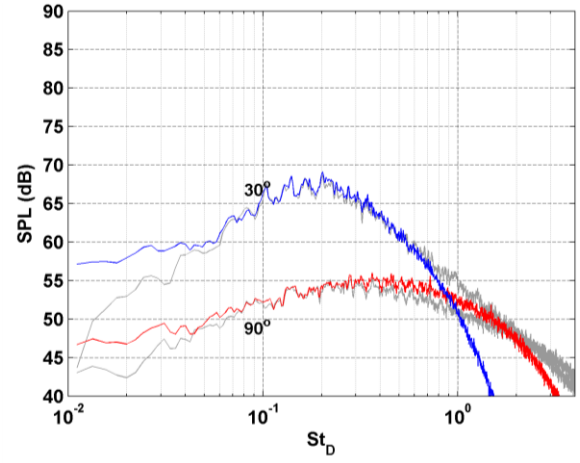

a) TTR = 1.0, Unexcited GDTL

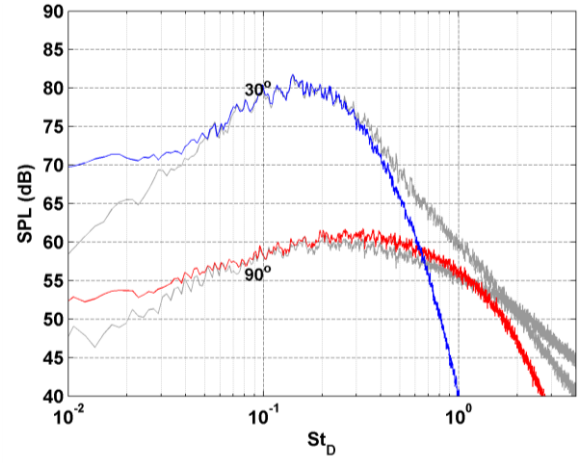

b) TTR = 2.0, Unexcited GDTL

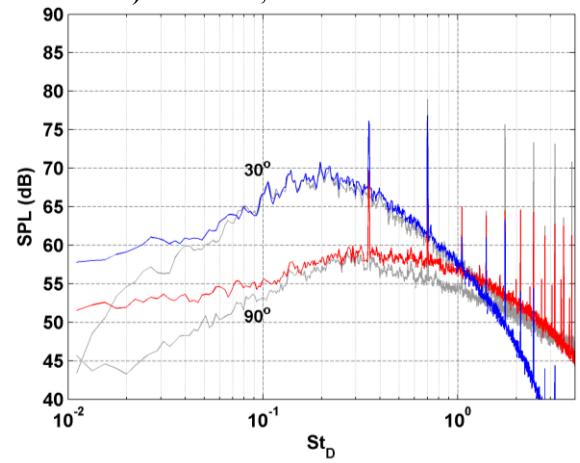

c) TTR = 1.0, m = 0, St_{DF} = 0.26

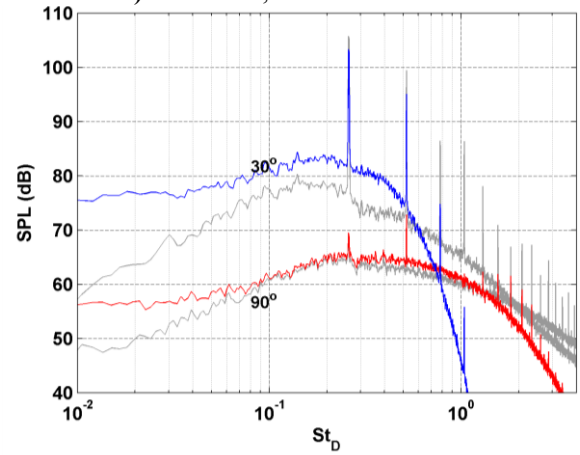

d) TTR = 2.0, m = 0, St_{DF} = 0.26

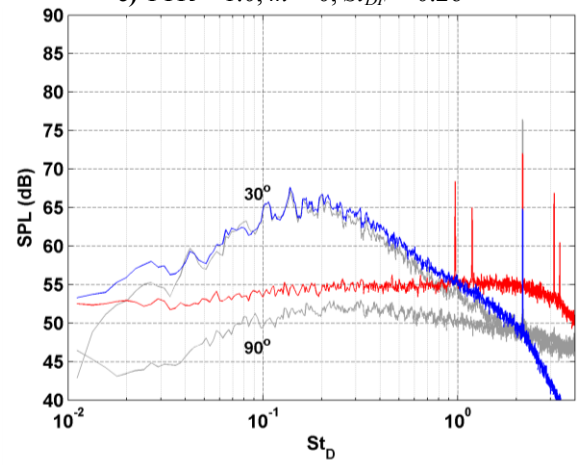

e) TTR = 1.0, m = 3, St_{DF} = 2.0

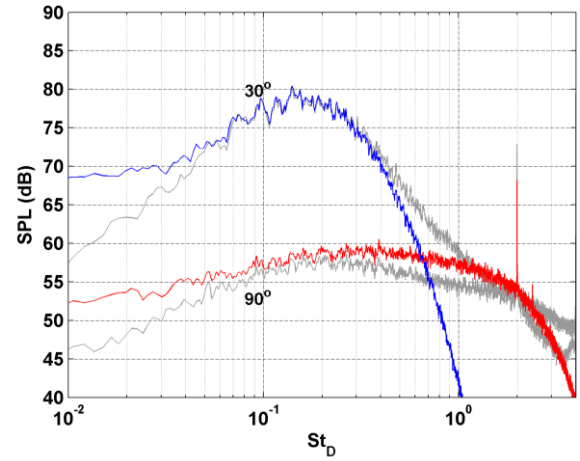

f) TTR = 2.0, m = 3, St_{DF} = 2.0

Fig. 5: Example spectra for signal reconstruction – colored spectra are reconstructions.

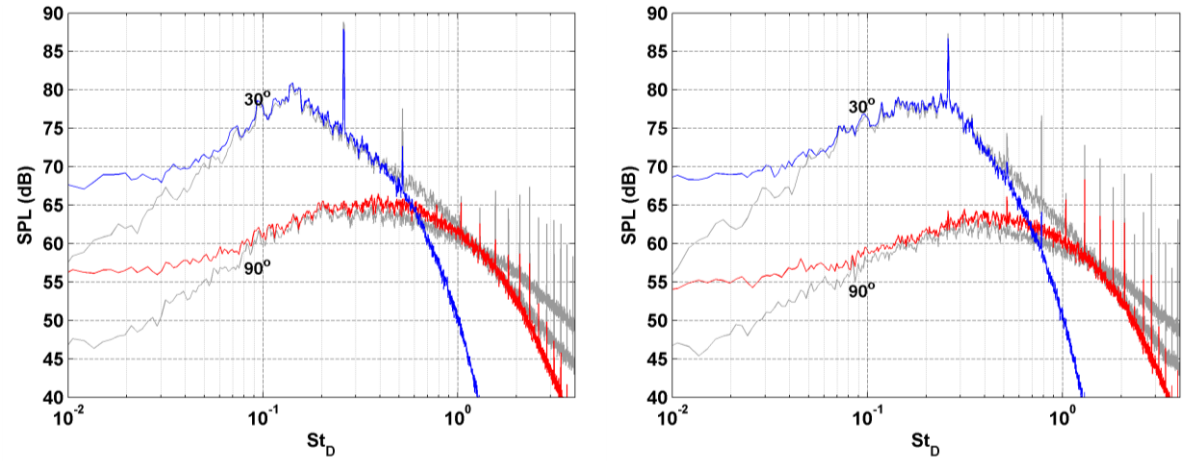

a) TTR = 2.0, m = 1, St_{DF} = 0.26 **b)** TTR = 2.0, m = 3, St_{DF} = 0.26

Fig. 6: Additional example spectra showing lack of over-prediction.

To understand how the spectral levels are being over-predicted in some of these cases, a portion of the reconstructed time-domain signal for one such case is shown in Fig. 7 – the data is plotted versus inverse Strouhal number. It should be noted that most excitation parameters produce time-domain signals and reconstructions that look similar to those in the previous work [6]. The change in signal characteristics responsible for the changes observed in the ΔOASPL maps and narrowband spectra is immediately apparent. When excited with these parameters in the elevated temperatures, the noise radiated to low angles becomes highly periodic (with a period matching the excitation frequency) containing long chains of high-amplitude events. This apparent resonance condition results in over-prediction of the event peaks because the model function exaggerates the resonance. It is possible to eliminate this over-prediction by using a different model function, but it would complicate the analysis by requiring a method of determining when the alternate model function was needed for very little benefit. The over-prediction doesn't impact any of the statistics discussed in §4.2 and it is also a convenient indicator for the occurrence of this phenomenon. The behavior of the time-domain signal supports the discussion of superdirective radiation in §4.1.1. While it is possible to conceptualize this noise signature being created by highly periodic vortex interactions, the characteristics match those of superdirective radiation very well.

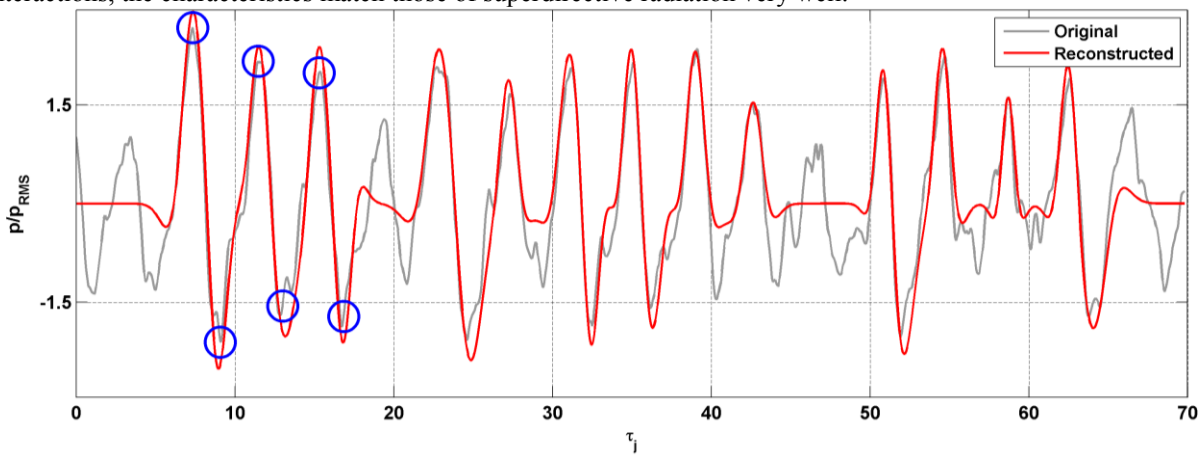

Fig. 7: Time-domain data for TTR = 2.0, m = 0, and St_{DF} = 0.26 at ϕ = 30°.

4.2 Statistical Analysis

Based on the spectral analysis of the excited jet (§4.1), it is concluded that the excited jet dynamics are fundamentally similar to the unexcited jet [6] with the few exceptions already discussed. The most relevant conclusion is that the statistical analysis of the events can focus on the low angles (30° is used) without missing important information. Additionally, the unexcited cases within the GDTL database do not need to be explored in great detail except for comparison purposes to excited cases. Since the unexcited jet results show that the statistics of

event width and intermittence have very similar behaviors, only the intermittence is discussed in detail and the mean width ($\overline{\delta t}$) is discussed in relation to the mean intermittence ($\overline{\Delta T}$).

4.2.1 Amplitude Distributions

The amplitude distributions for the excited jet are examined by focusing on 30°. The spectral analysis results (§4.1) will inform the discussion to further reduce the number of cases that need examining. The probability density functions (PDFs) for the peak amplitudes of extracted events are shown in Fig. 8 for all excitation frequencies at modes 0 & 1 and temperature ratios of 1.0 and 2.0. The distributions, for the most part, are very similar to the unexcited jet [6]. There are two notable differences in the excited jet results. In the unheated jet, it can be seen that the higher frequencies (the redder curves) are skewing toward the unit normal distribution for both modes. This variation is relatively slight and, given the likelihood that the data has a large amount of actuator self-noise as already discussed (§4.1.1), it is not likely that it is a meaningful variation. At the elevated temperature cases (TTR = 2.0) shown in Fig. 8, the departure from the unexcited distribution is associated with the strong increases in the OASPL. In mode 0, the low excitation frequencies (blues) have an amplitude distribution close to the unit normal while mode 1 has no such trend. This change is likely associated with a basic change in the nature of the typical event created by exciting with these parameters. As discussed in [6], the unexcited event amplitude distributions skew away from the unit normal because the peaks only contain part of the information about points above the $1.5p_{RMS}$ threshold. The typical event in these highly excited cases, however, is different from the typical event in most other cases. As seen in Fig. 7, these cases are characterized by periodic high-amplitude oscillations. The peaky characteristics of these events mean that the peak amplitude is more representative of the data above the threshold so it recovers a distribution close to the unit normal—the distribution of the total signal (see [6]). While not shown, the other polar angles, temperatures, and azimuthal modes have amplitude distribution characteristics consistent with a combined interpretation of the unexcited results and the range of excitation frequencies and polar angles where the strong amplification occurs.

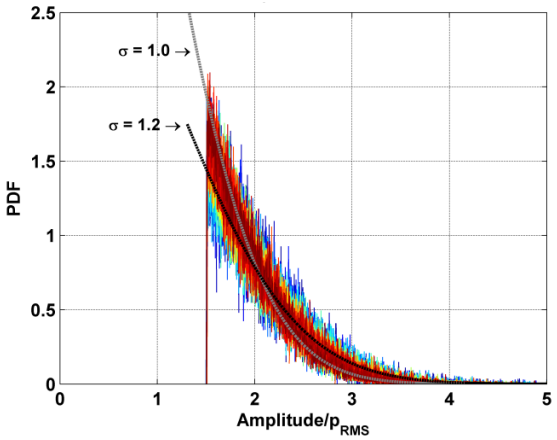

a) TTR = 1.0, m = 0

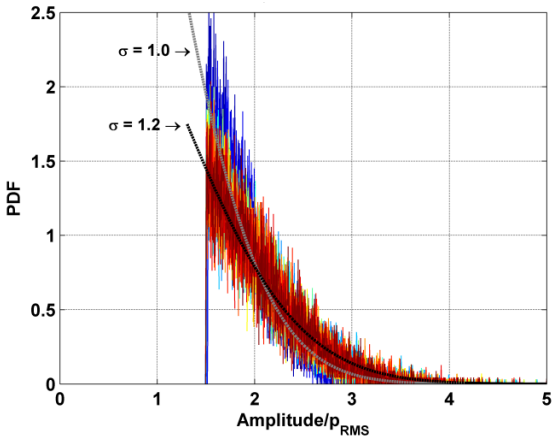

b) TTR = 2.0, m = 0

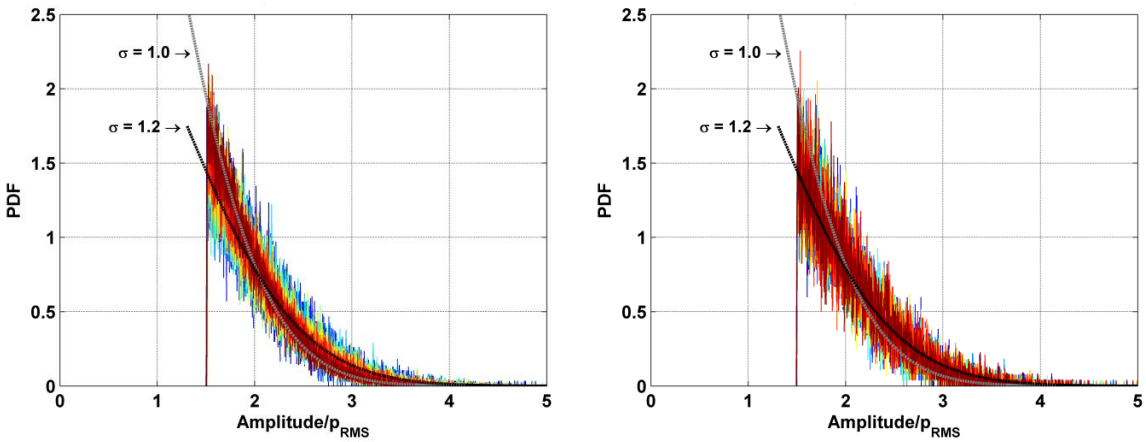

c) TTR = 1.0, m = 1 **d)** TTR = 2.0, m = 1

Fig. 8: PDF of peak amplitudes for all excitation frequencies at ϕ = 30°. Higher frequencies are in red and lower frequencies in blue.

4.2.2 Intermittence Distributions

The amplitude distributions indicate that, in most cases, the excited jet statistics are likely to behave similarly to the unexcited jet. Therefore, to get an overall picture of the intermittence distribution behaviors without presenting an unwieldy number of plots, the following metric is used to describe how much a particular case deviates from the unexcited distribution. The distributions are normalized by their respective means as done in [6]. The best fit gamma distribution for the unexcited data (baseline) is determined for a given operating condition and polar angle. The Root Mean Square (RMS) error of a particular distribution with respect to the baseline best fit gamma distribution is computed. Finally, this RMS error is normalized by the RMS error of the baseline distribution with respect to its own best fit gamma distribution. In this way, quantities significantly greater than one indicate a distribution that is a meaningful departure from the baseline while removing the expected changes in the distribution that occur due to a changing mean. This quantity is referred to as the "gamma deviation."

The gamma deviation for two temperature ratios at four polar angles (ϕ = 30°, 45°, 60°, & 90°) are shown in Fig. 11 for all the forcing cases under study. Looking at the unheated case, it is clear that all of the azimuthal modes show substantial deviation from a gamma distribution over a wide range of frequencies. The deviation has generally similar levels regardless of azimuthal mode, but there is some directional dependence. At the low angles where the jet is loudest, the deviation is generally weaker. The deviation becomes more prominent as the angle increases; presumably because the baseline jet noise is lower at the larger angles allowing the actuator self-noise to more easily dominate. The TTR = 2.0 jet case is quite different. Modes 1 and 3 have very little deviation except for a small amount at the sideline angles for high excitation frequencies. Mode 0, in contrast, shows a very strong localized deviation that correlates very well with the excitation frequency and directivity characteristics of the large OASPL increase already discussed (§4.1.1). The other polar angles and temperatures (not shown) have behaviors and trends consistent with the results shown. The TTR = 1.5 case behaves like the TTR = 2.0 case implying that the diminution of the self-noise problem occurs somewhere between TTR = 1.0 and TTR = 1.5. The indiscriminant deviation with respect to excitation frequency in the unheated case supports the previous conclusion that actuator self-noise is a prominent feature at this operating condition.

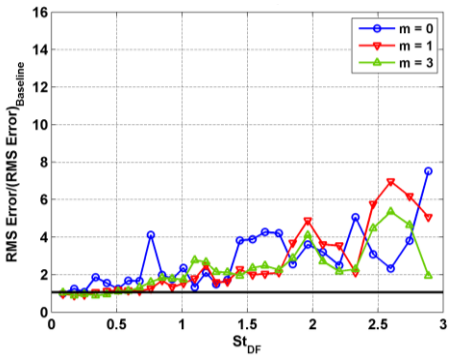

a) TTR = 1.0, ϕ = 30°

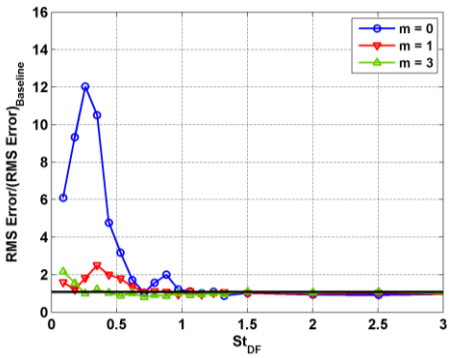

b) TTR = 2.0, ϕ = 30°

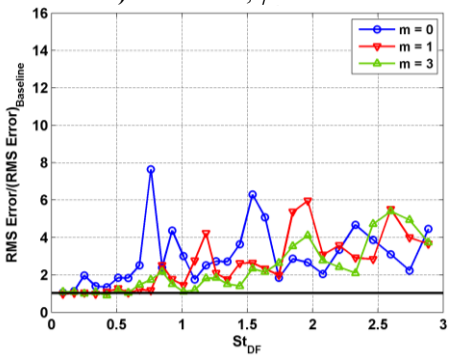

c) TTR = 1.0, ϕ = 45°

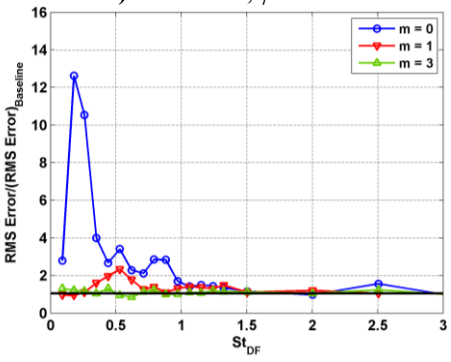

d) TTR = 2.0, ϕ = 45°

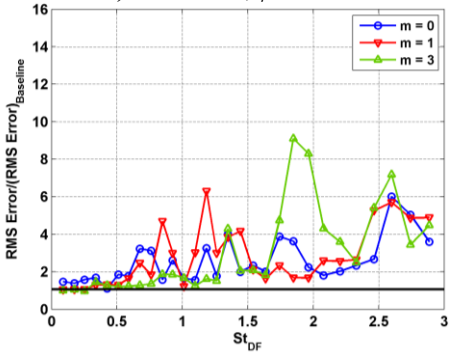

e) TTR = 1.0, ϕ = 60°

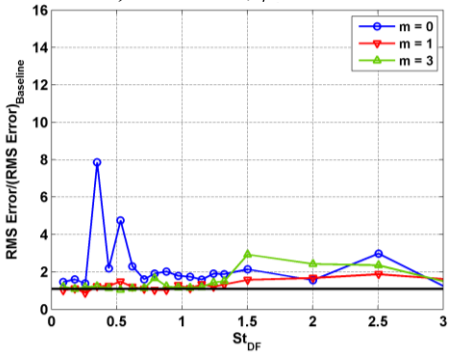

f) TTR = 2.0, ϕ = 60°

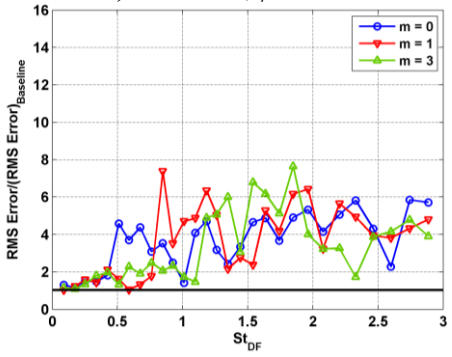

g) TTR = 1.0, ϕ = 90°

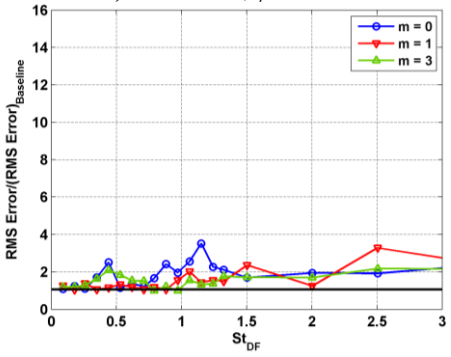

h) TTR = 2.0, ϕ = 90°

Fig. 9: Gamma deviations for temperature ratios of TTR = 1.0 & 2.0 and ϕ = 30°, 45°, 60°, & 90°.

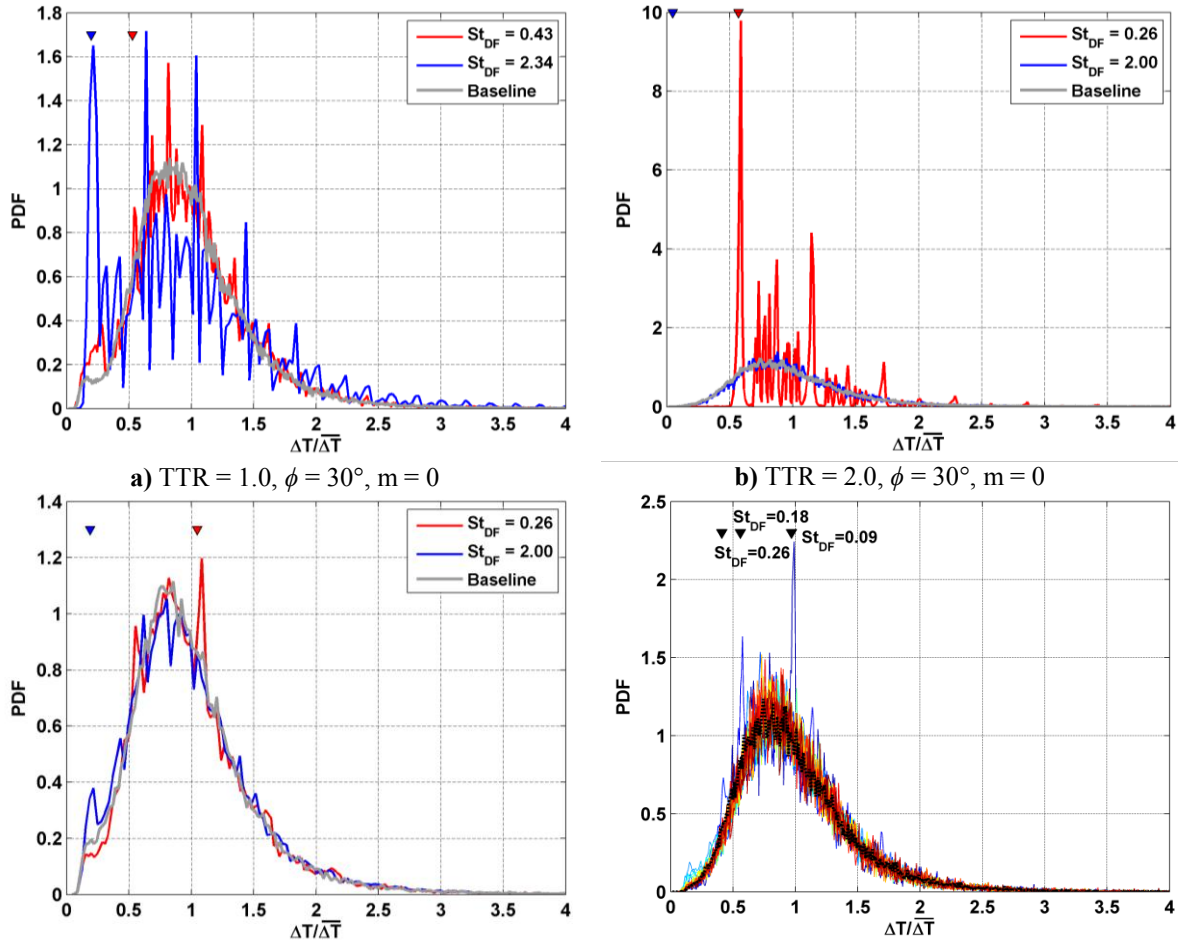

a) TTR = 1.0, ϕ = 30°, m = 0

b) TTR = 2.0, ϕ = 30°, m = 0

c) TTR = 2.0, ϕ = 60°, m = 0

d) TTR = 2.0, ϕ = 30°, m = 3

Fig. 10: Intermittence distributions normalized by their respective means for the excited jet.

Several examples of the intermittence distributions are shown in Fig. 10 to illustrate the different characteristics indicated by the gamma deviation. Note that these distributions are normalized by their respective means consistent with previous analysis [6]. In each of these figures, the unexcited intermittence distribution (Baseline) is shown as a black or gray line and the excitation periods are indicated by downward pointing triangles.

In the cold jet at ϕ = 30° excited with mode 0 (Fig. 10a), the deviation at low excitation frequencies is due to narrowband spikes that are multiples of the excitation period. The distribution at these conditions retains the same basic shape as the baseline so the gamma deviation values are near one. At the higher excitation frequencies, the intermittence distribution is being significantly altered. Very strong spikes are visible (multiples of the excitation period) and these cause the shape of the distribution to flatten resulting in large gamma deviations.

Looking at the same polar angle and excitation mode but at an elevated temperature (Fig. 10b) reveals just how radically the distribution is being altered by excitation. For low excitation frequencies near the jet column natural frequency ($St_D \approx 0.3$), the distribution is dominated by a spike at the excitation period with weaker spikes at multiples of the fundamental period. The occurrence of events with these few periodicities is so high that the remaining portions of the distribution have negligibly small probabilities. For the same conditions at large excitation frequencies, however, the distribution is indistinguishable from baseline. To look at directivity, the intermittence distributions at ϕ = 60° are shown (Fig. 10c) for the same temperature and excitation parameters as (Fig. 10b). It is clear that the distribution deviates only slightly from the baseline due to excitation with the strongest deviation being a narrowband spike associated with the excitation period when that period is near the natural mean period. Finally, to examine the excitation mode response, the intermittence distributions for mode 3 (Fig. 10d) are shown for the same polar angle and temperature as (Fig. 10b) with one exception. In (Fig. 10d), the distributions are plotted for all the excitation frequencies. It is clear that exciting this mode does not create strong deviations from the baseline

distribution. There are a few narrowband spikes at the fundamental periods for a few of the lower excitation frequencies, but the distribution shape is essentially unchanged.

These distributions show that the gamma deviation is indeed a good descriptor of changes in the distribution shape. Additionally, this result adds support to the conclusion that the jet at the elevated temperatures is generating strong superdirective radiation when excited with the axisymmetric mode near the jet column natural frequency.

4.2.3 Mean Width and Intermittence

Based on the unexcited jet analysis [6], the mean width and intermittence are parameters governing the changes in the jet noise signal characteristics. Additionally, a strong link between these two quantities was observed in the unexcited jet ($\overline{\delta t}/\overline{\Delta T}$ = 0.128). That same scaling is applied to the data in this section to see if the behavior is preserved under excitation and to minimize the number of needed figures.

The unexcited (Baseline) mean quantities for the GDTL data are shown in Fig. 11. Comparing these data to the unexcited database [6], there are some similarities and some differences. It should first be noted that the scaling factor of 0.128 between the mean event width and intermittence is consistently a good scaling in the GDTL data. Looking at the unheated case (TTR = 1.0)—for which a nearly direct comparison exists in Case 4 of the unexcited work [6]—the distributions are very similar. The mean width at ϕ = 30° is nearly identical between the two databases; as is the trend to the sideline angles. The mean width at ϕ = 90° is slightly lower in the GDTL facility, but it is unlikely that the discrepancy is significant. The previous discussion of the sideline angles [6] showed that the noise event analysis is of very limited use at the sideline and upstream angles. Additionally, the idea that noise radiated to the sideline comes from fine-scale turbulence dictates that differences in things like nozzle geometry, boundary layer turbulence, etc. should result in differences in the noise production. The only discrepancy of note in the unheated case is the behavior at ϕ = 25°. In the unexcited data [6], the event width continues increasing with decreasing polar angle. The GDTL data, however, changes direction below ϕ = 30°. This is most likely a facility dependence in the GDTL created by the location of the ϕ = 25° microphone within the anechoic chamber. The ϕ = 25° microphone is located in a corner of the anechoic chamber in relatively close proximity to the walls and the collector – the data in the unexcited work [6], in contrast, has no such proximity issue. It is therefore likely that noise reaching this microphone is being altered by this proximity; thus discussion of the data at ϕ = 25° should be minimized.

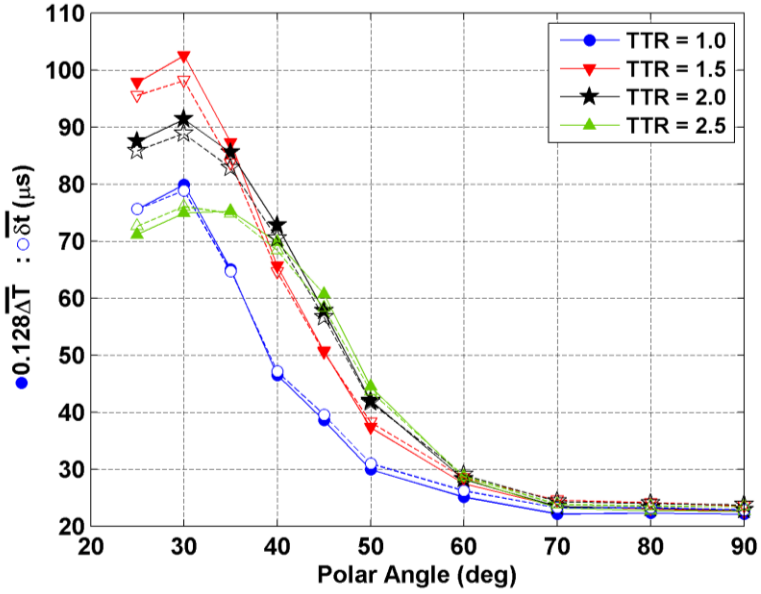

Fig. 11: Mean width and intermittence for the unexcited jet data from GDTL.

The trend with increasing jet temperature in the GDTL database is a much more complex comparison. The GDTL database holds a fixed hydrodynamic Mach number while varying the stagnation temperature ratio while the previous work [6] holds the acoustic Mach number constant while varying the exit temperature ratio. The result is that the approach in the previous work isolates temperature as a variable while holding the jet velocity constant whereas the GDTL approach results in a coupled change in the jet velocity and temperature. The approach of the

previous work is therefore superior for hydrodynamically subsonic jets, but is not practical for supersonic jets due to the additional complexities of a supersonic flow. At the time of collection, this best practice was not known to GDTL – otherwise the data would have been collected following the best practice. One consequence of this is that the GDTL jet becomes acoustically supersonic (as seen in Table 1) and previous work has shown that Mach wave radiation is emerging as a significant noise source in the higher temperatures of the jet currently under discussion [69]. The onset of an additional noise source complicates the picture, but the previous work indicates that it should be a relatively weak contribution in terms of the acoustic spectra. Looking at the transition (ϕ = 40° to 60°) and sideline angles, the trend with increasing temperature in the GDTL data is similar to the unexcited previous work [6]. The low angles, however, have a trend that is similar to the previous work for the lower temperatures, but that reverses direction for the two highest temperature ratios. Unless compressibility effects, created by the combined increase in temperature and velocity, are producing changes in the source mechanisms of the mixing noise sources, it is likely that this behavior is indicative of the presence of Mach wave radiation, but that the Mach wave radiation source is too weak to produce any significant changes in the spectral shape. This result dictates that any significant changes in excitation response between TTR = 1.5 & 2.0 or TTR = 2.0 & 2.5 at the low angles, must be discussed with the possibility of competing noise sources in mind.

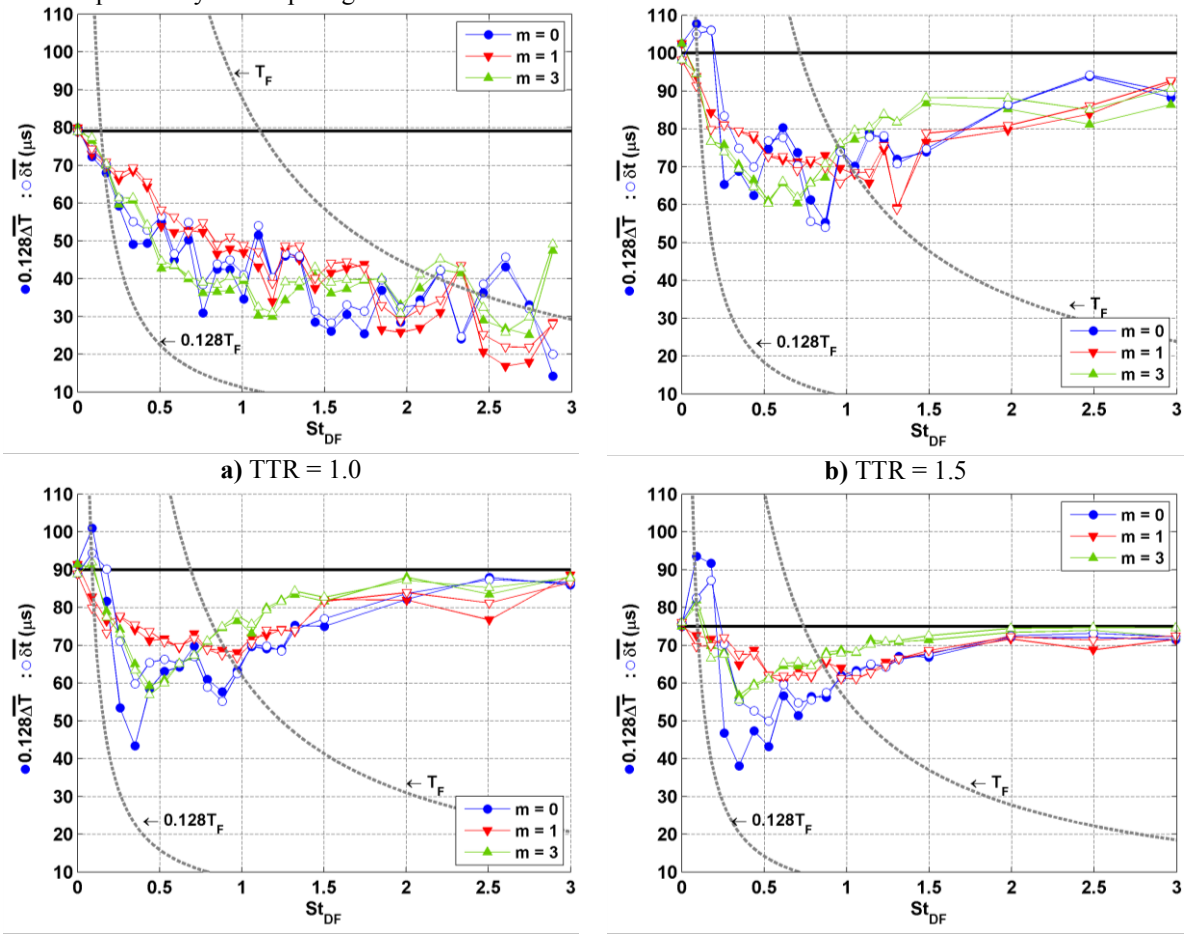

a) TTR = 1.0 **b)** TTR = 1.5

c) TTR = 2.0 **d)** TTR = 2.5

Fig. 12: Mean width and intermittence for various temperatures at ϕ = 30°. T_F is the excitation period.

The mean width and intermittence for ϕ = 30° are shown in Fig. 12 for the four temperature ratios. The excitation period (T_F) is also shown in these figures for context. Looking at the cold jet first, it can be seen that the scaling of 0.128 is held quite well regardless of excitation parameters at this temperature. Again there is evidence that the data has significant actuator self-noise: the azimuthal modes are indistinguishable and trend consistently downward to smaller and smaller intervals with increasing excitation frequency. It is difficult to say from the data, but it appears that the mean event width is asymptotically approaching the excitation period. Comparing these data to the ΔOASPL data (Fig. 5a) offers very little insight except to confirm the indistinguishable nature of the different azimuthal modes at this temperature.

At a temperature ratio of 1.5, the behavior of the changes in the mean width and intermittence are starkly different from those of the unheated jet. The different azimuthal modes trend down to some minimum and then trend back toward the baseline levels with increasing excitation frequency. This reinforces the idea that the jet is being excited without overwhelming the acoustic field with actuator self-noise. It is also clear in this case that the different azimuthal modes are affecting the mean quantities in different ways.

In mode 0, the mean intermittence closely follows the excitation period for excitation frequencies less than $St_{DF} \approx 0.3$ as might be expected from the previous discussions. Even at the lowest excitation frequencies measured, the noise source dynamics are still so strongly controlled by the excitation that the intermittence increases above the baseline. It should be remembered, however, that the relationship between the intermittence distribution and the mean is strained in these strong response cases (i.e. $m = 0$ at elevated temperatures with $St_{DF} \leq 0.6$). When the baseline distribution is obliterated by a strong periodicity, the mode of the distribution will be the best descriptor. As already discussed (§4.2.2), the mode of the distribution in these strong response cases is exactly the excitation frequency. This explains why the mean intermittence in these cases follows the excitation frequency while not matching it. Since these strong response cases constitute only a small portion of the parameter-space, the mean of the distribution is still better than the mode as a general descriptor of the changes in the distribution in response to excitation. The amplification of the OASPL peaks when the excited mean intermittence matches the baseline (at an excitation frequency of $St_{DF} \approx 0.2$). This frequency is close to the spectral peak frequency of the low-angle noise. This strongly suggests the idea that the excitation frequency is matching a naturally occurring resonance. Another observation of mode 0 excitation is that, for the low frequencies ($St_{DF} < 0.6$), the changes in mean width are smaller than the changes in the intermittence. This suggests that, while the dynamics governing the width and intermittence are strongly related, the behavior of one does not necessarily determine the exact behavior of the other. There are two local minima in the excitation intermittence response, $St_{DF} \approx 0.4$ & 0.8, at TTR = 1.5 & 2.0. As the temperature increases, the minimum at 0.8 vanishes. The locations of these minima are, roughly speaking, harmonics of the spectral peak frequency. Given that the jet responds very strongly to exciting at the spectral peak frequency with mode 0, it makes sense that strong responses might also be observed at harmonics of that fundamental.

The changes induced by exciting modes 1 and 3 aren't as dramatic as mode 0. In these modes, there is always good agreement between the width and intermittence. Mode 1 has a gradual trend with a large flat trough – the peak noise reduction occurs somewhere in this bottom. Mode 3 has a more pronounced minimum with noise reduction peaking at excitation frequencies just larger than the intermittence minimum. Apart from the change in behavior between the unheated and TTR = 1.5 cases that is attributable to the dominance of actuator self-noise, there aren't any readily identifiable significant changes in the excitation response with increasing temperature. It is therefore concluded that the additional noise source of Mach wave radiation is not a significant factor in the jet noise (at least with respect to excitation response) at these conditions.

For completeness, the mean width and intermittence data at $\phi = 90°$ are shown for two representative temperature ratios in Fig. 13. In the unheated jet, the issue of actuator self-noise is readily apparent – the mean width approaches the limits of the signal resolution (10 μs) and doesn't trend back toward the baseline at the high excitation frequencies (Note that only the scaled intermittence values ever dip below 10 μs). The elevated temperature case does trend back toward the baseline. The event width and intermittence are always well matched by the 0.128 scaling and there is no detectable difference between the azimuthal modes. If the data at this polar angle has anything meaningful to say, it is that exciting the jet makes the oscillations in the sideline noise even more rapid.

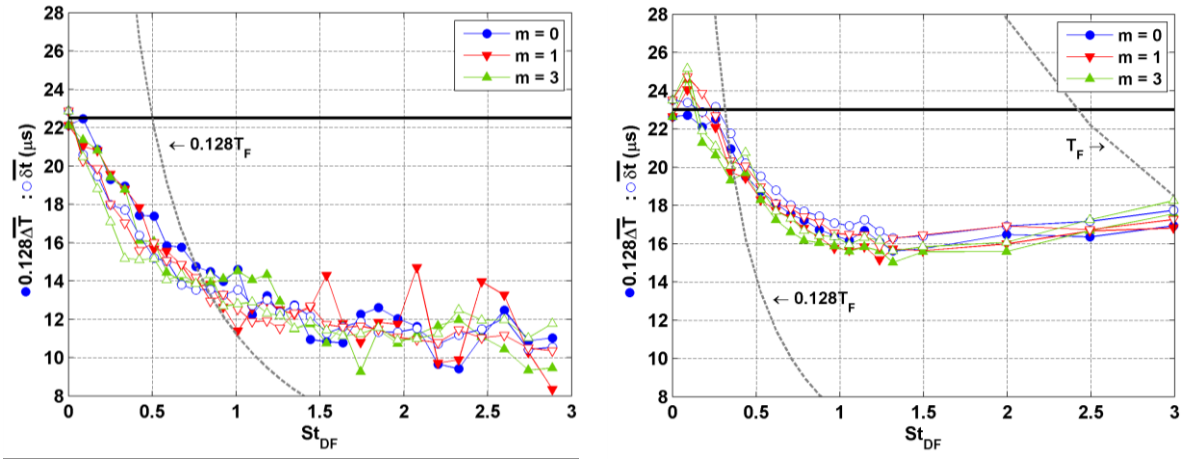

a) TTR = 1.0 **b)** TTR = 2.0

Fig. 13: Mean width and intermittence for two representative temperatures at $\phi = 90°$.

The behavior of the jet in response to excitation frequency and azimuthal mode suggest a process of competition, both in the temporal axis (which is highly correlated with the axial direction) and the azimuthal axis. One of the general results is that significant noise reduction occurs when the excitation period is smaller than the induced mean intermittence, and also larger than the event width. The maximum noise reduction occurs when the induced mean intermittence period is roughly five times greater than excitation period. Studies of the flow-field (see references discussed in §2.2) have shown that excitation at these frequencies generates a single structure for each pulse of the actuator. If the mean intermittence doesn't match the excitation period, the implication is that only some of the structures are producing noise events. It appears that the noise sources radiating to the low angles (i.e. large-scale structures) are competing for flow energy. Noise reduction occurs when excitation produces an environment in which this competition limits the amount of energy that any one structure can consume. Conversely, noise amplification occurs when excitation tunes the jet to allow each structure to consume as much energy as possible. This idea will be discussed more in §6.

4.2.4 Joint PDF—Amplitude and Width – 30°

Before examining the response to excitation, it is prudent to look at the distributions of the unexcited cases from the GDTL database to see if there are differences relative to the unexcited results discussed in [6]. The joint PDFs for the 30° microphone are shown in Fig. 14 for the four temperature ratios. On the whole, the distributions from the GDTL database are quite similar to the previous results. The main difference is that the elongation with heating is more pronounced in the GDTL facility. It is difficult to say if this difference is a facility dependence or is due to heating while holding the hydrodynamic Mach number fixed. Given the high degree of similarity between the most closely matched unheated cases (Fig. 14a and Fig. 10a in [6]) however, it is more likely that this difference is the result of holding the hydrodynamic Mach number fixed. As discussed in [6], the elongation with increasing temperature indicates that the width and amplitude are becoming less correlated.

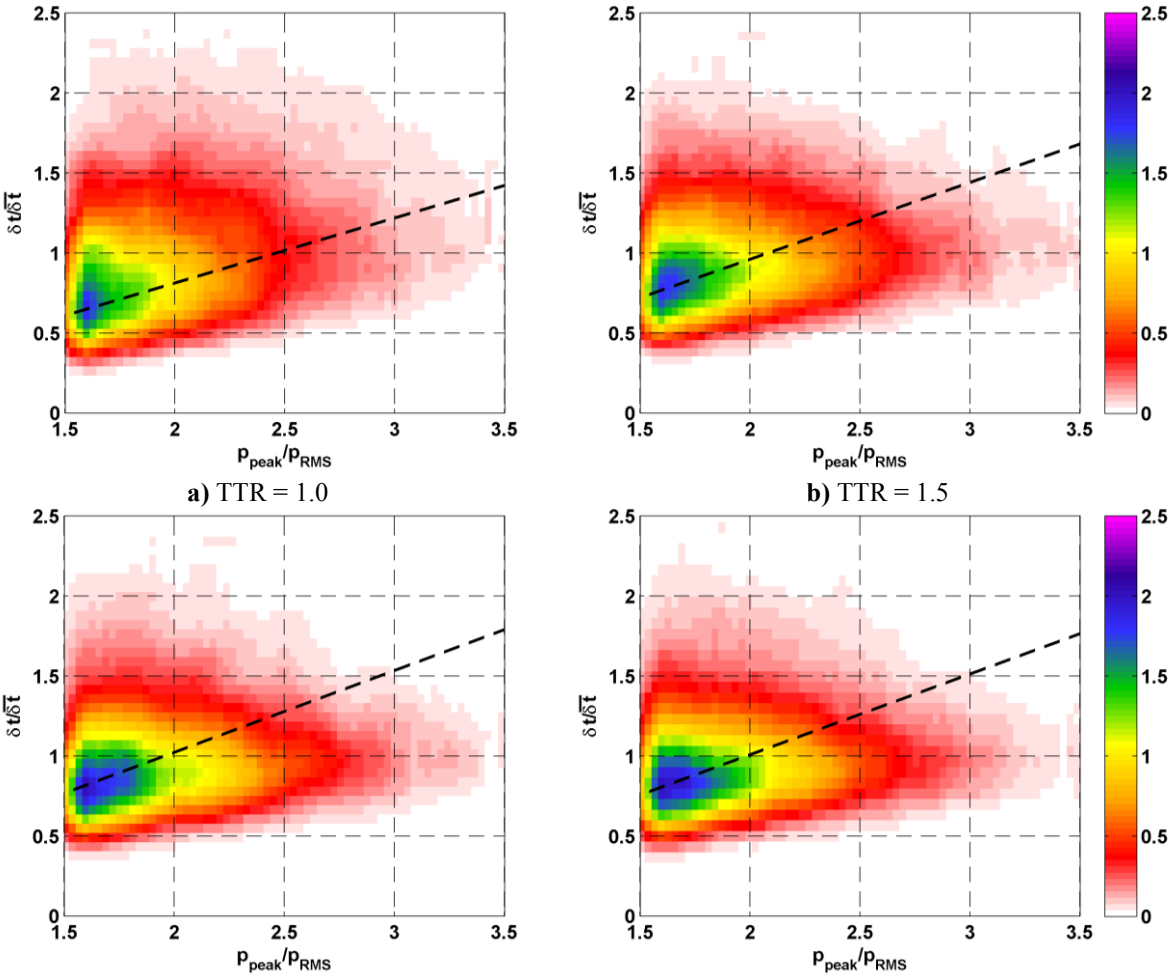

a) TTR = 1.0 **b)** TTR = 1.5

c) TTR = 2.0 **d)** TTR = 2.5

Fig. 14: Unexcited joint-PDFs of amplitude and width from the GDTL data at various temperature ratios at $\phi = 30°$.

In the interest of keeping the number of figures to a reasonable level, a few select excited distributions at a temperature ratio of TTR = 2.0 are shown in Fig. 15. In addition to the doubling line, the excitation period is marked with a black triangle on the right-hand edge of the figures. As already discussed, the results at a temperature ratio of TTR = 1.0 seem to have significant levels of actuator self-noise. It is decided that it is sufficient to present one temperature ratio as representative of the joint PDF characteristics given the likelihood of a small benefit for a large number of additional figures required to present multiple temperature ratios. Excitation azimuthal modes 0 and 3 are shown because they elucidate the characteristic behaviors and the frequencies chosen highlight significant points in the trends. While not shown, the trends and behaviors discussed here are also seen in the temperature ratio 1.5 and 2.5 data.

Looking at the distributions, it is clear that $m = 0$ is creating much more significant changes. As expected at this point from the other results, exciting the jet with $m = 0$ near $St_{DF} = 0.2$ radically reshapes the distributions. What is interesting about this distribution is that width is apparently independent of the amplitude when excited in this resonant regime. Additionally the width distribution is almost symmetric about the mean width. The distribution is also much more compact. These characteristics are all consistent with the results already discussed. As the excitation frequency increases (Fig. 15b) the distribution trends back toward a shape similar to the unexcited jet. As the excitation period passes through the mean width (Fig. 15 c & d), the distribution becomes bimodal in the event width; the second lobe is a harmonic of the primary lobe. By the time $St_{DF} = 3.0$ is reached, the distribution has returned to the baseline.

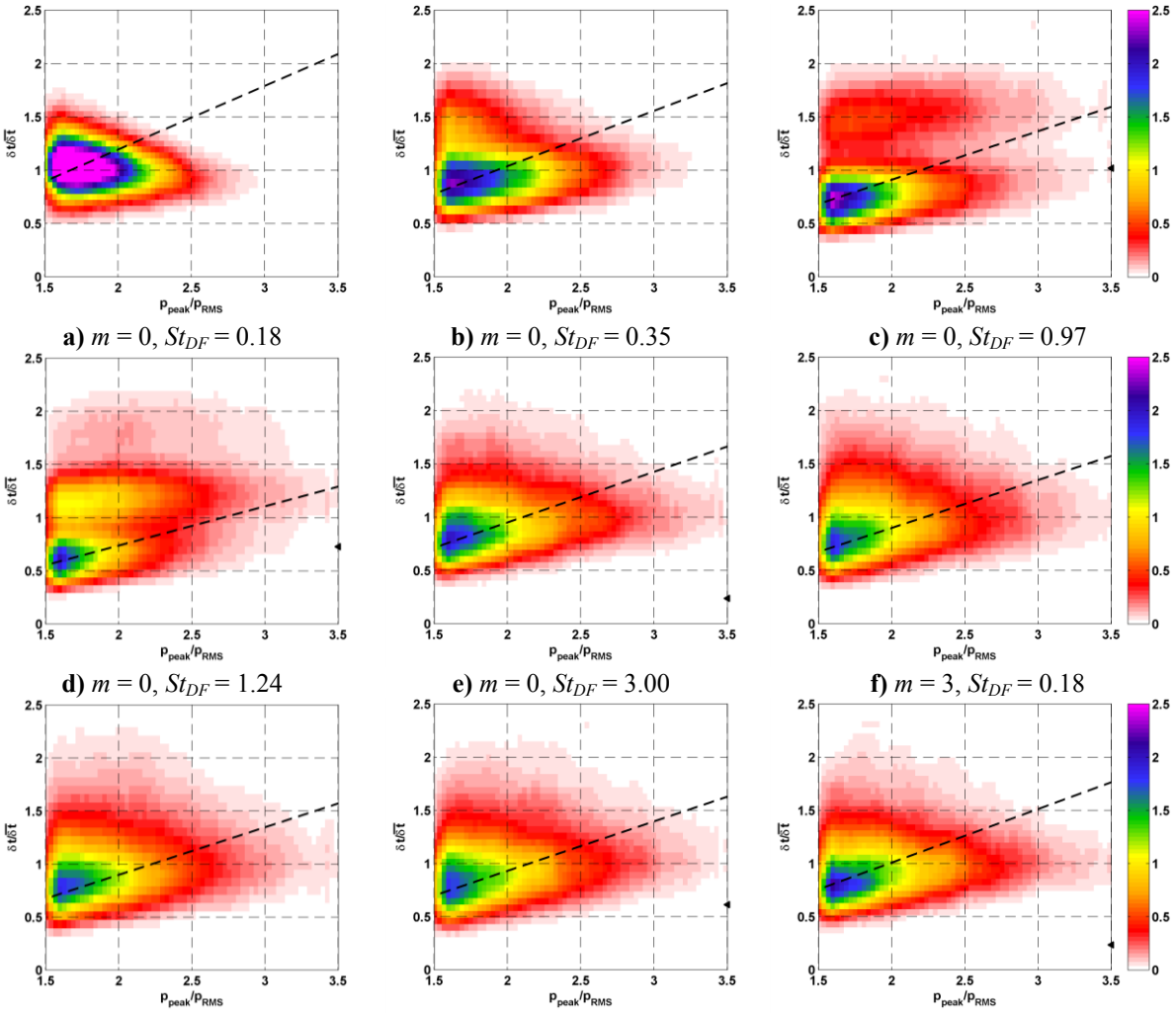

a) $m = 0$, $St_{DF} = 0.18$ **b)** $m = 0$, $St_{DF} = 0.35$ **c)** $m = 0$, $St_{DF} = 0.97$

d) $m = 0$, $St_{DF} = 1.24$ **e)** $m = 0$, $St_{DF} = 3.00$ **f)** $m = 3$, $St_{DF} = 0.18$

g) $m = 3$, $St_{DF} = 0.35$ **h)** $m = 3$, $St_{DF} = 1.24$ **i)** $m = 3$, $St_{DF} = 3.00$

Fig. 15: Joint-PDFs for several excited cases at TTR = 2.0 and $\phi = 30°$.

Azimuthal mode 3 is much less complicated than mode 0. The distribution characteristics are essentially unchanged by excitation. This is consistent with the results from preceding sections. The information from these joint-PDFs agrees with the other analyses and additionally shows a link between amplitude and width. Given the complexity of the link between the two quantities, however, it would be difficult to reduce to an analytical expression without over-simplifying the dynamics.

4.3 Summary of Results

As already established in previous publications [52] and briefly discussed in §4.1.1, the plasma actuators are capable of manipulating jet noise. The spectral analysis shows that:

1. The reduction/amplification characteristics depend on jet temperature, excitation frequency and azimuthal mode, and polar angle.
2. The quantitative amount of far-field acoustic energy that can be removed through excitation increases with increasing temperature.
3. The excitation tone amplitude of $m = 0$ at the low angles ($\phi < 50°$) increases at elevated temperatures for excitation Strouhal numbers near the jet column natural frequency ($St_D \approx 0.3$). Close inspection reveals that the greatest increase occurs at the excitation frequency of $St_{DF} = 0.18$ – near the spectral peak frequency. This suggests, based on the unexcited results [6] that link the mean intermittence to the spectral peak frequency, that exciting the jet with mode 0 at that frequency reinforces the naturally occurring events. These changes in the tone amplitude create large changes in the OASPL that occur only in mode 0. This is

highly suggestive of strong superdirective radiation and its onset at elevated temperatures is likely related to the disproportionate growth of mode 0 energy in the jet when the temperature is elevated.

4. Actuator self-noise appears to be a significant contribution to the noise signature in the unheated jet, but becomes inconsequential at elevated temperatures because the jet gets louder.
5. While difficult to determine from the lower temperatures alone, the complete picture indicates that $m = 3$ produces the largest decreases in the OASPL and that these decreases occur at the lowest angles measured ($\phi = 25°$ & $30°$).
6. The excitation Strouhal number that removes the most energy at the low angles decreases with increasing temperature and is different for the different azimuthal modes. Mode 0 settles near $St_{DF} \approx 1.3$, while modes 1 and 3 settle at $St_{DF} \approx 0.5$.
7. Strong reduction at the low angles is accompanied by amplification at the higher angles. Uniform reduction is achievable when exciting at high frequencies, but the reduction is quantitatively smaller than peak reduction levels. Also, there isn't any well-defined optimum excitation frequency or azimuthal mode for reduction at the high forcing frequencies.

The statistical analysis based on noise-event identification provides the following additional insights.

1. Actuator self-noise is a problem in the statistical metrics of the unheated jet – reinforcing the conclusion from the spectral analysis.
2. In most cases, the statistical description of the jet noise (i.e. the shape of the distributions) is not being significantly changed by excitation.
3. When excited in the strongly resonant regime (i.e. $m = 0$ and $St_{DF} \approx 0.1$-0.5 at elevated temperatures), the naturally occurring (i.e. unexcited) statistical distributions of the event intermittence are totally obliterated by a single intermittence interval equal to the forcing period. This suggests that the excitation is achieving a resonance with the natural frequencies of the jet – supported by the fact that the strongest resonance occurs when the induced mean intermittence matches the baseline mean intermittence and that this matching occurs when the jet is excited with frequencies roughly matching the spectral peak frequency ($St_{DF} \approx 0.2$).
4. The relationship between the mean intermittence ($\overline{\Delta T}$) and width ($\overline{\delta t}$) as determined from the unexcited jet ($\overline{\delta t}/\overline{\Delta T} = 0.128$) is still valid in the excited jet with one exception. In the strongly resonant regime, the mean width is not as strongly affected compared to the mean intermittence. This divergence in the relationship between these two quantities suggests that the mechanisms responsible for these characteristics are linked, but that one does not always dictate the exact nature of the other.
5. The nature of the jet response, both in terms of frequency and azimuthal mode, suggests a process in which noise sources are competing for flow energy. Noise reduction occurs when excitation produces a competitive environment that limits the amount of energy that any one structure can consume – limiting a structure's ability to produce a noise event. Conversely, noise amplification occurs when excitation tunes the jet to allow each structure to consume as much energy as possible – resulting in large noise events.

The most probable cause for the increasing amounts of noise reduction with increasing temperature is the rapid growth in the energy of the $m = 0$ mode as the temperature is elevated [70, 71]. Results supporting the observations about the behavior of mode 0 with regard to LAFPAs are presented in Kearney-Fischer *et al.* [53]. It is generally believed that the axisymmetric mode is the most efficient radiator of sound [74] – this idea is strongly supported by the present work. If the competition process is indeed present, the highly organized perturbations seeded by exciting higher azimuthal modes (e.g. $m = 3$) grow and consume as much of the available flow energy as possible. Consequently, there is less energy available for the $m = 0$ mode. Thus, the unexcited heated jet converts more energy into sound than the unheated jet, but when excited, the energy conversion is severely suppressed by diverting that energy into modes which are less efficient radiators. However, reduction achieved with mode 0 excitation indicates that there must also be a contribution from the highly organized nature of the excited structures. Given the apparent resonance conditions in which mode 0 excitation can produce large increases in noise, it makes sense that some noise reduction could be achieved in mode 0 by exciting the jet away from the resonance condition (i.e. frequencies considerably larger than $St_{DF} = 0.2$) as long as the frequency isn't so high that the jet is unresponsive.

The strong superdirective radiation created by exciting the axisymmetric mode suggests that the spatial coherence of the structures plays an important role. A possible explanation for the intermittent nature of low-angle noise would then be that temporal fluctuations in the spatial coherence of the large-scale structures produce periods of increased radiation efficiency. The characteristic frequency of the wave-packet would then be associated with the event width and frequency of the events would be related to the frequency of the coherence fluctuations. This idea is further explored in §6.2.

5 MEASUREMENTS OF STRUCTURE INTERACTION

The results discussed in §4 highlighted questions about the behavior and interaction of the large-scale structures in the jet (both in terms of the excited jet behavior and also what that infers about the unexcited jet). The two most important observations are the discussion of a resonance condition and the idea that structures may be competing for flow energy. While there are many questions that could be explored regarding the nature of the structure interaction, the two most critical are:

1. What is the impulse response of the jet? This question is important because it looks at the behavior of a structure in isolation and can answer other questions such as 'can a large-scale structure exist in isolation or does it require adjacent structures to support its growth?' The impulse response of the jet is something that has not been well studied in the literature. The explorations of jet or shear layer excitation in the literature usually focus on the response to single frequency excitation and then sweep that frequency [e.g. 29].
2. Can evidence of competition for flow energy be found and what is the behavior of that competition?

In an effort to address these questions, GDTL has begun experiments using excitation and a linear microphone array placed in the near-field hydrodynamic region. The jet is excited with frequencies ranging from very low (250 Hz or $St_{DF} = 0.02$) to moderate Strouhal numbers ($St_{DF} = 1.4$). Exciting the jet at very low frequencies is equivalent to exciting the jet with a single pulse because all of the timescales of the jet are very small compared to the excitation period. The perturbation produced by LAFPAs is much more similar to a delta function than a sinusoid. A single pulse from these actuators is then a very good tool for studying the impulse response of the jet. Studying the impulse response of the jet, as well as the signature of the large-scale structures over a wide range of frequencies, can provide support for the speculation on structure behavior in the preceding sections. To date, only the axisymmetric mode has been explored so conclusions will be somewhat limited. These experiments are ongoing, but the results to date have some very relevant conclusions. This work is discussed in detail in another paper from GDTL [75] (presented at this conference) so only some applicable results are presented here. The jet examined here is the same Mach 0.9, $D = 2.54$ cm, unheated jet (TTR = 1.0) studied in §4. While it was shown that actuator self-noise was a problem in the acoustic far-field, the amplitude of the hydrodynamic pressure fluctuations is much higher so actuator self-noise is not a significant problem.

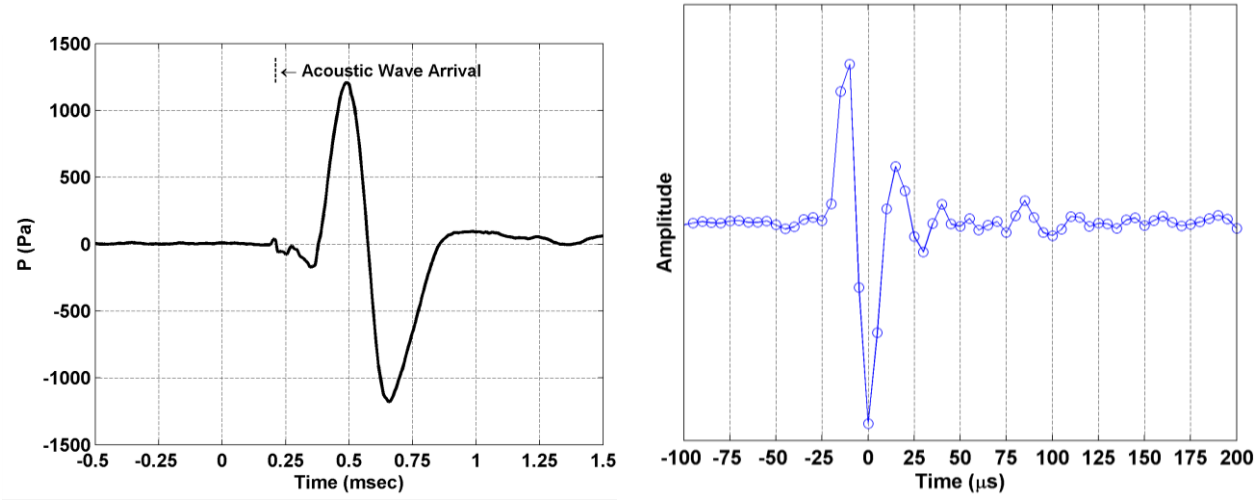

a) $m = 0$ Impulse Response **b)** Actuator acoustic wave in quiescent air

Fig. 16: The single pulse behavior of the jet and the actuator acoustic wave.

The impulse response of the jet to axisymmetric excitation is shown in Fig. 16a. Technically, the jet is excited with $m = 0$ at 250 Hz ($St_{DF} = 0.02$), but this frequency is low enough to be considered synonymous with the impulse response as will be confirmed. In this figure, time equals zero corresponds to the rising edge of the actuator control signal. The impulse response signal shown in Fig. 16a is the average of about 1000 pulses. Examining the impulse response, several features are apparent.

1. The acoustic wave from the actuators (i.e. the actuator self-noise) arrives at about 0.22 milliseconds which is consistent with the time taken to traverse the three jet diameters at the speed of sound in the

ambient air. It is clear that the actuator self-noise is quite weak in comparison to the signature of the large-scale structure. The averaged acoustic wave from a single actuator firing in quiescent air is shown in Fig. 16b (the abscissa has its zero aligned with the primary peak because the time of flight from the actuator to the far-field isn't relevant to this discussion). The microphone is far enough from the actuators that the compression wave, which initially steepens and strengthens [76], has relaxed into an acoustic wave.

2. The large-scale structure signature consists of one low-pressure lobe and one high-pressure lobe. Both features must be present since the pressure field of the jet must be isobaric in a net sense.
3. The pressure minimum arrives at about 0.65 milliseconds and the entire event lasts about 0.6 milliseconds.

While the width and depth of the negative lobe can be associated with the size and energy of the large-scale structure, these quantities change with axial and radial location so they can't, as such, be directly useful in a discussion of the jet noise dynamics. These characteristics will be further discussed in the context of interaction. This clearly indicates that large-scale structures do not require the existence of adjacent structures to grow. While the vast body of previous work relating jet noise to instability waves of a given frequency (e.g. typical wave packet models) can be and is still useful, this result supports the previous conclusion cautioning against the use of such an approach when the basic constituents of the dynamics are not of a fundamentally periodic nature.

One consequence of the impulse response nature of the jet is that, for excitation frequencies low enough to keep the structures separated, the energy per unit time should add independently and be directly related to the excitation frequency (see [75] for more discussion of structure superposition). Based on the impulse response duration of about 0.6 milliseconds, this would correspond to a frequency of about 1.67 kHz (St_{DF} = 0.15). Relating St_{DF} = 0.15 to a spatial distance using U_c = $0.6U_j$ results in $\Delta x = 0.6\,D/St_{DF} \rightarrow \Delta x = 4D$. For excitation frequencies higher than this, it is expected that interaction and competition for energy should take place. To get an overview sense of this, the mean square pressure of the phase-averaged signals at various excitation frequencies is calculated and normalized by the jet exit kinetic energy density (Fig. 17). The unexcited mean square pressure (Baseline) is marked for reference. The line associated with the independent addition of energy, using the impulse response energy as the reference point, is also shown. Just as expected, the excitation frequencies below about St_{DF} = 0.15 very closely follow the independent addition line. This confirms that the signature associated with exciting at St_{DF} = 0.02 is indeed representative of the impulse response. Beyond this frequency, the energy per unit time continues to increase, but starts to fall away from the independent addition line. The energy per unit time peaks at St_{DF} = 0.25 and then decays rapidly – falling below the baseline levels by a Strouhal number of about St_{DF} = 0.45.

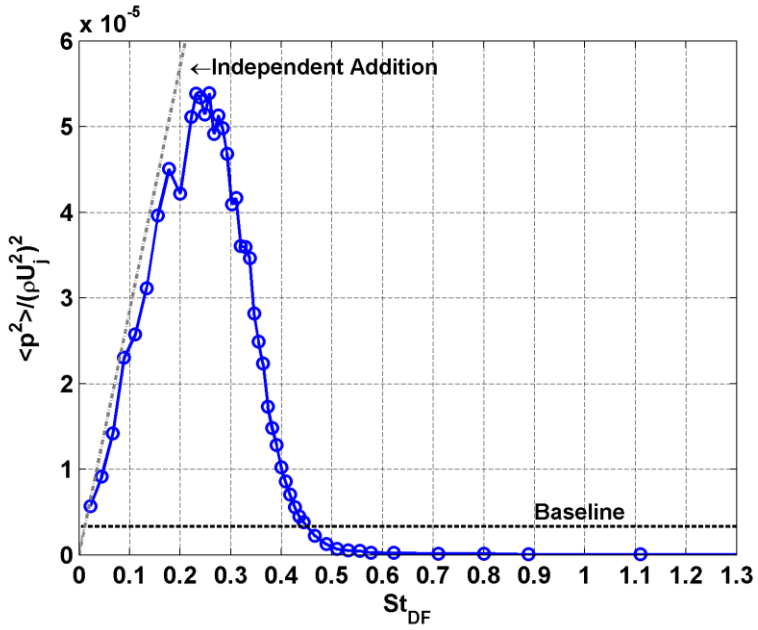

Fig. 17: Mean square pressure of the phase-averaged pressure signal for axisymmetric excitation at various frequencies.

To get a better sense for how the structures are being affected, several examples are shown in Fig. 18. For each example, the phase-averaged signal is shown along with the impulse response signal and the excitation period is marked by a black bar. The first example (St_{DF} = 0.13) is the highest frequency for which the adjacent impulse responses (including the actuator acoustic wave) don't appreciably interact. It can be seen that, at this and any lower excitation frequency, the structures do not interact in an appreciable way. The second example (St_{DF} = 0.26) shows how the structures start interacting when the energy per unit time is maximized. The amplitude of the signal is unchanged from the impulse response, but the adjacent structures are compressing one another slightly resulting in an almost perfectly sinusoidal shape. The next example (St_{DF} = 0.35) shows a case where the interaction of the structures has started to inhibit structure growth. The amplitude is reduced and the structures are increasingly compressed (remember that the time axis of these data are directly related to spatial extent by way of the convective velocity of the structures). In the last example (St_{DF} = 0.49), the inhibition of structure growth by competition has become quite severe. The expected periodicity is still present, but the amplitude and shape of the structure signature is significantly altered.

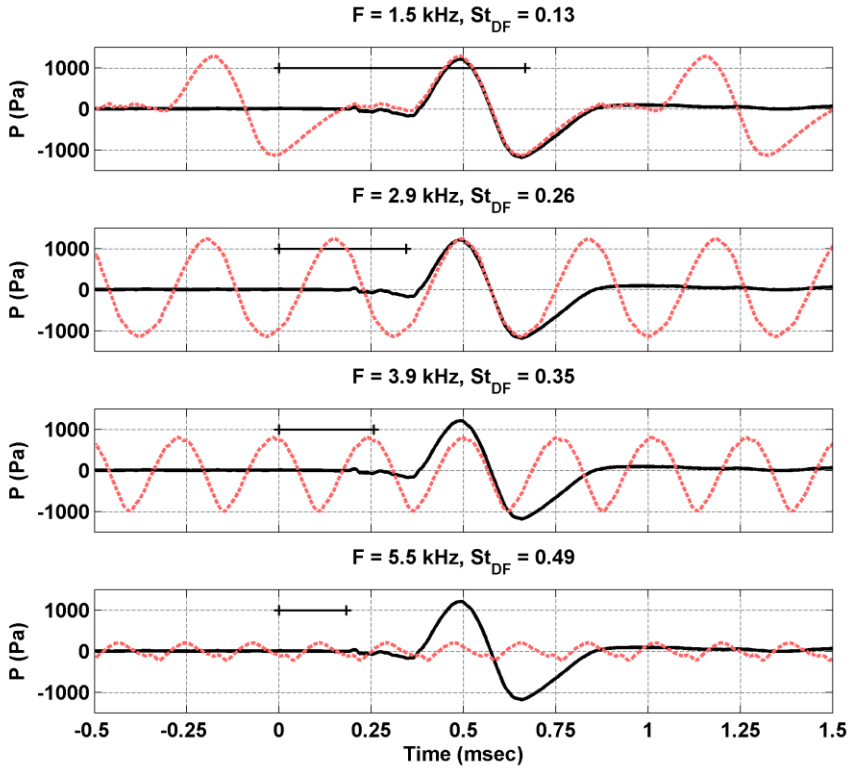

Fig. 18: Examples of the large-scale structure signature for various excitation frequencies.

These results reveal several important aspects about large-scale structure behavior and interaction in the jet. As seen in these data, as well as previous experiments using LAFPAs (§2.2), excitation produces one structure per excitation period over a wide range of frequencies – at this point it could be said that this statement is true over the range $St_{DF} = 0$ to $St_{DF} \approx 1.5$. The size and energy of a structure is only dependent on the frequency for frequencies greater than $St_{DF} \approx 0.15$. For frequencies greater than this threshold, the structures interact, first in a way that increases the energy density (i.e. energy per unit time), but then in a competitive manner that inhibits the ability of the structures to extract energy from the flow. The frequency that results in the greatest energy density ($St_{DF} = 0.25$) is in the same region as the postulated resonance phenomenon discussed in §4. While the numbers don't line up exactly, they are quite close and factors such as temperature have not been taken into account at this point.

Turning these conclusions toward the unexcited jet reveals the following. Structures that are separated by at least a sufficient distance in space ($\Delta x \approx 4D$) have similar energy per structure, but greater separation equates to less energy per unit time. As the structure spacing approaches resonance ($St_{DF} \approx 0.2 \rightarrow \Delta x \approx 3D$), the maximum energy per unit time is reached. Beyond resonance, the structures compete for energy and drag down the energy per unit time. As long as the energy radiated to the far-field is even loosely related to the energy of the structures (a

conclusion supported by all of the other results), this distribution of energy provides an explanation for why the most energy in the acoustic far-field is associated with the resonance frequency.

While not discussed in detail here, the preliminary results to date have shown that the structure characteristics scale in time as Strouhal number and in amplitude with the jet exit kinetic energy density. These scaling parameters were used in the preceding discussion and are validated by results presented in [75]. Since it is not known how the impulse response changes with temperature, excitation azimuthal mode, etc., the conclusions discussed here cannot be considered finalized, but they are significant nonetheless.

6 THE IMPLICATIONS FOR NOISE SOURCES

Previous works (§2.2) showed that there are separate structures for each excitation pulse from each actuator and that, under the right conditions (exciting near the jet column natural frequency $St_{DF} \approx 0.3$), neighboring structures will merge into larger structures and grow to large energies/sizes before disintegrating. Under other conditions ($St_{DF} \approx 0.6$-1.5 depending on azimuthal mode), excitation creates structures that initially grow rapidly, but then stop growing and convect in a stable manner before breaking up.

The analysis of noise events shows that a resonance exists in the jet – evidenced by the large noise amplification that occurs when the jet is excited at a frequency matching the mean intermittence of the unexcited jet. In this case, at least in a statistically averaged sense, every large-scale structure produces a noise event. Additionally, it was found that very strong amplification occurred when the jet was excited axisymmetrically (i.e. $m = 0$). This analysis also showed that significant noise reduction occurs when only a fraction of the large-scale structures produce noise events. These results suggest a process in which noise sources are competing for flow energy and that these noise sources are closely related to the large-scale structures. These results divide into two areas: a general behavior of competition, and the specific impact of azimuthal extent.

6.1 The Competition Model

Based on the experimental results, a descriptive model encompassing the observed behaviors is now discussed. There are two aspects to this model that dictate noise production: the interaction of structures, and the intrinsic energy within a structure. Within a range of excitation frequencies, the amount of interaction between neighboring structures is controlled by the excitation. Obviously, the azimuthal mode of excitation dictates the interaction in the azimuthal dimension. If the frequency is too low, the jet naturally produces structures in between those generated by excitation. When the frequency is too high, the jet statistics trend back toward the baseline (see §4.1.1). It may be that the actuator amplitude is diminishing at these high frequencies or that the jet doesn't convert the perturbations into individual structures (likely attributable to some combination of diminished Kelvin-Helmholtz instability growth rates and vortex merger/dissipation processes), but excitation does seem to alter the jet in small ways (implying that these high frequencies are at least subtly altering the naturally occurring structures).

The energy contained within a structure is controlled by both the excitation and the Shear Layer Instability (SLI). The SLI (as discussed in §2.2) preferentially amplifies a range of frequencies. At low excitation frequencies, the SLI amplifies the perturbation generated by each pulse as a totally independent event (i.e. the impulse response) and will amplify the perturbation according to the amplification rates inherent in the instability. When the excitation frequency is sufficiently high, the SLI won't amplify the perturbations as independent events and this will change the way in which the initial perturbations are amplified. The details of this behavior were discussed in §5.

The size and the energy of a structure are related – as should be expected. As shown in the work of Kambe *et al.* [e.g. 7], the size of a structure impacts the time-scale of the noise event (i.e. width) produced by a vortex collision. While the dynamical link isn't clear at this point, it is important to acknowledge that the energy of a structure beyond its size is also likely to be a parameter on the generation of noise events.

The idea of structure competition has been discussed in a previous work from GDTL [77] on non-ideally expanded supersonic jets. In that work, it was observed that the excited structures had to compete with the naturally occurring structures for flow energy. In a non-ideally expanded supersonic jet, a strong feedback loop is established by the interaction of the large-scale structures and the shock-train that naturally excites structures in a periodic fashion at frequencies near the jet column natural frequency. This feedback process generates a tonal noise called screech noise. This work showed that the range of excitation frequencies that produced robust structures was reduced compared to an ideally expanded jet and that the structure passage frequency in the jet would vacillate

between the screech frequency and the excitation frequency. This is strong evidence that structures can and do compete for flow energy and provides precedent for the ideas discussed here.

Putting the results and the preceding discussion into an enumerated form, the model of the noise sources is as follows.

1. Premises
   - 1.a. The dynamics of the large-scale structures are at least causally linked to the noise events.
   - 1.b. A structure must have certain characteristics to generate a noise event (most probably, it may need to have absorbed enough energy from the flow – this would be manifest in the structure's size, rotational kinetic energy, etc.).
2. The process by which a noise event is generated.
   - 2.a. A perturbation is seeded (naturally or artificially), rolls up into the beginnings of a structure, and the structure starts to develop.
   - 2.b. Depending on its proximity to other structures, the structure in question will develop in different ways. To facilitate this description, the axial and azimuthal separations are divided into a few categories: Axial separation (FAR $\rightarrow$ $St_{DF} < 0.1$, RESONANT $\rightarrow$ $St_{DF} \approx 0.2$, CLOSE $\rightarrow$ $0.5 < St_{DF} < 1.5$), Azimuthal separation (FAR $\rightarrow$ $m = 3$, CLOSE $\rightarrow$ $m = 0$ or 1).
     - 2.b.i. Axial – FAR, Azimuthal – FAR: Each structure develops with characteristics dictated by the impulse response of the SLI. This case results in a relatively benign structure that convects and dies without producing a strong noise event.
     - 2.b.ii. Axial – FAR, Azimuthal – CLOSE: The structures azimuthally merge into a single structure whose characteristics are still dictated by SLI, but that has greater ability to extract energy out of the flow (especially if the structure is azimuthally complete – e.g. $m = 0$). This case has structures with more energy than 2.b.i, but the structures occur infrequently so they don't result in significant energy per unit time reaching the far-field.
     - 2.b.iii. Axial – RESONANT, Azimuthal – FAR: Neighboring structures reinforce each other and can grow to energies larger than those seen in cases 2.b.i or 2.b.ii, but are still relatively restrained by the confined azimuthal extent. This case produces well organized structures, but the confined azimuthal extent of the structures still largely limits the potential to produce strong noise events.
     - 2.b.iv. Axial – RESONANT, Azimuthal – CLOSE: Neighboring structures merge into an azimuthally cohesive structure and axially neighboring structures reinforce each other. This case produces well organized structures with the largest energies and the strongest noise events.
     - 2.b.v. Axial – CLOSE, Azimuthal – FAR: Axially neighboring structures compete with one another for flow energy; limiting their ability to grow. One consequence of these competing structures is that they prevent more energetic structures from developing. This case produces well organized, but reduced energy structures compared to 2.b.iv. These structures don't produce particularly strong noise events, and they also prevent more energetic structures (that would produce strong noise events) from forming.
     - 2.b.vi. Axial – CLOSE, Azimuthal – CLOSE: Axially neighboring structures compete with each other (as in 2.b.v), but the azimuthal merger process still allows them to pull out more energy from the flow in comparison to 2.b.v. This case is not substantially different from 2.b.v, but its noise events will be somewhat stronger.
     - 2.b.vii. Final note: If the excitation frequency is too high ($St_{DF} > 1.5$), the instability dynamics simply stop generating structures one-to-one with excitation. This places a limit on how closely structures can be packed and also says that this limit is imposed by the flow dynamics.
   - 2.c. The structure decays due to viscous forces further downstream or disintegrates due to collisions with itself or other structures near the end of the jet potential core.

There are several important observations to be made about this model. In the unexcited jet, a mix of all these cases occur, but since those of 2.b.iv produce the strongest noise events, the far-field spectrum has its peak associated with this periodicity. In the reality of case 2.b.i, the jet will produce other structures in between the ones in question whereas 2.b.v doesn't allow other structure patterns to occur – this is why exciting the jet into the 2.b.v configuration results in noise reduction while low frequency excitation doesn't have any effect on the statistical noise picture. Exciting in the 2.b.v regime eliminates the 2.b.iv events that sometimes occur in the unexcited jet, but the rough shape of the spectrum isn't radically changed because the 2.b.iv events-only occur sometimes in the unexcited jet and the broadband shape of the spectrum is dictated, in large part, by the width of the noise events. Lastly, there is a balance that must be struck between the amplitude and the frequency of noise events. This model suggests that, as the structure frequency increases, the number of noise events per unit time will increase

proportionally. The model also says that the strength of those noise events changes with frequency. As expected, noise reduction is achieved when these two factors are tuned so that the energy per unit time reaching the far-field is less than that of an uncontrolled jet.

6.2 The Relationship Between Azimuthal Extent and Radiation Power

As discussed in §4.3, the excited jet results showed that the azimuthal extent of the structures plays a significant role in the low-angle noise. One method for exploring this issue is through a superdirective noise model [e.g. 73]. In this case, the noise source is modeled as lying on a cylinder whose radius is the same as nozzle radius (R). Using a simple model for the axial fluctuations, the noise source term can be written as

$$T_{11}(\underline{y},\tau) \propto R\delta(r-R)\exp\left[i(\omega\tau - k\, y_1) - y_1^2/\lambda^2\right]C_n e^{in\theta}, \tag{1}$$

where θ is the azimuthal coordinate, R is the jet radius, and there is an implied summation over all integers n (i.e. Einstein notation). Since the azimuthal content is described as a Fourier series, any azimuthal distribution can be represented.

The solution to Lighthill's equation using only the T_{11} source term with the far-field assumption in cylindrical coordinates is

$$p(\underline{x},t) = \frac{\cos^2\phi}{4\pi|\underline{x}|a_\infty^2}\frac{\partial^2}{\partial t^2}\int_{-\infty}^{\infty}\int_0^{2\pi}\int_0^{\infty} T_{11}\left[\underline{y}, t-|\underline{x}-\underline{y}|/a_\infty\right] r\, dr d\theta dy_1. \tag{2}$$

It can be assumed without loss of generality that the azimuthal coordinate of the observer is zero. Using this assumption, the distance between the source and observer in the far-field in cylindrical coordinates is approximately

$$|\underline{x}-\underline{y}| \approx |\underline{x}| - y_1\cos\phi - R\cos\theta\sin\phi. \tag{3}$$

Inserting the source term and evaluating the trivial radial integration, the far-field pressure is

$$\begin{aligned} p(\underline{x},t) \propto{}& \frac{R^2\cos^2\phi}{4\pi|\underline{x}|a_\infty^2}\frac{\partial^2}{\partial t^2}\exp\left[i\omega(t-|\underline{x}|/a_\infty)\right]\times \\ & \int_{-\infty}^{\infty}\exp\left[i(\omega\cos\phi/a_\infty - k)y_1 - y_1^2/\lambda^2\right]C_n dy_1 \int_0^{2\pi}\exp\left[i\omega R\cos\theta\sin\phi/a_\infty\right]e^{in\theta}d\theta. \end{aligned} \tag{4}$$

Inspection reveals that the primary difference between (4) and its one-dimensional model equivalent (not shown) is the appearance of a factor containing the azimuthal integral – as should be expected. This integral is of the form of Bessel's first integral so it can be evaluated as

$$\begin{aligned} \Theta_n &= \int_0^{2\pi}\exp\left[i\omega R\cos\theta\sin\phi/a_\infty\right]e^{in\theta}d\theta \\ &= 2\pi i^n J_n\left[\omega R\sin\phi/a_\infty\right] \\ &= 2\pi i^n J_n\left[\pi St_D M_a\sin\phi\right], \end{aligned} \tag{5}$$

where J_n is the n^{th} order Bessel function of the first kind. If ($\pi\, St_D\, M_a \sin\phi$) ≈ 0, all $J_n \approx 0$ except for J_0 so only the axisymmetric sources can radiate when the argument of the Bessel function is small unless this factor is offset by the Fourier coefficients – a result noted by Cavalieri *et al.* [58]. This is mathematical support for the idea that the axisymmetric mode is the most efficient radiator of low-angle jet noise – at least within the scope of these simple models. Equation (5) also indicates that the axisymmetric mode is the most efficient radiator for low Strouhal numbers regardless of polar angle, but it must be remembered that the polar angle directivity is dictated by other factors in the model. This result provides a possible explanation for the experimental results showing that exciting the axisymmetric mode with low Strouhal numbers results in strong amplification. Since it is possible for the azimuthal Fourier coefficients (C_n) to be functions of t or y_1, the coefficient factor must be left inside the axial integral and time derivatives of (4). If C_n are not functions of t or y_1, the far-field pressure is the product of the result from the one-dimensional model and the azimuthal factor $C_n\Theta_n$:

$$p(\underline{x},t) \propto A[\underline{x}]\exp\left[i\omega(t-|\underline{x}|/a_\infty)\right]C_n\Theta_n, \tag{6}$$

where all of the various purely real valued factors have been aggregated into A for compactness.

In order to make a meaningful assessment of the contribution of varying azimuthal extent, it is necessary to assume a model of the azimuthal extent. While a time and space-varying model would be the most representative, that level of complexity rapidly becomes analytically intractable. Therefore, a model that is independent of both t and y_1 will be used. A simple model for the axial extent is a Gaussian with the scale parameter (β). As $\beta \to \infty$, the Gaussian models an axisymmetric (i.e. $m = 0$) source while small values for β model azimuthally confined sources. Without loss of generality, the peak of the Gaussian can be placed at $\theta = 0$. The Fourier coefficients of the Gaussian are

$$\begin{aligned} C_n &= \frac{1}{2\pi}\int_{-\pi}^{\pi} e^{-\theta^2/\beta^2} e^{-in\theta} d\theta \\ &= \frac{\beta}{4\sqrt{\pi}}\left(\operatorname{erf}\left[\frac{\pi}{\beta} + \frac{in\beta}{2}\right] + \operatorname{erf}\left[\frac{\pi}{\beta} - \frac{in\beta}{2}\right]\right) e^{-n^2\beta^2/4}. \end{aligned} \tag{7}$$

It can be shown that all of the coefficients (C_n) are real and that $C_n = C_{-n}$; as should be expected from the transform of a real even function. In order to put the width of the Gaussian on a more physical footing, β is defined as

$$\beta \equiv \frac{\pi\,\delta\theta}{\sqrt{\ln[2]}}, \tag{8}$$

so that $\delta\theta$ is the percentage of the azimuth with an amplitude greater than ½.

The properties of the Fourier coefficients of the Gaussian allow for additional simplification of the far-field pressure (6). The summation over the Fourier components can be separated into a real and imaginary portion,

$$C_n \Theta_n = M_{\text{even}} + iM_{\text{odd}}, \tag{9}$$

where M_{even} & M_{odd} are the summations over the even and odd terms respectively. Incorporating this result into (6) and retaining only the real portion, the far-field pressure is

$$p(\underline{x},t) \propto A[\underline{x}]\left\{\cos\left[\omega\left(t - |\underline{x}|/a_\infty\right)\right] M_{\text{even}} - \sin\left[\omega\left(t - |\underline{x}|/a_\infty\right)\right] M_{\text{odd}}\right\}. \tag{10}$$

Only the real part is retained because, based on the utilization of a complex exponential representation of a travelling wave, only the real part represents the physical solution. The imaginary part is retained through the preceding calculation steps because of the mathematical convenience of complex numbers. From (10) it can be seen that the acoustic power in the far-field is

$$W_p = \frac{1}{A^2 T}\int_0^T p^2 dt = \frac{1}{2}\left[M_{\text{even}}^2 + M_{\text{odd}}^2\right], \tag{11}$$

where T is the period of the far-field signal and the power has been normalized by A^2 so that the quantity W_p is a dimensionless representation of the energy contribution from only the azimuthal factor. Strictly speaking, the factor of ½ in (11) comes from the integration of the trig functions. In order to numerically evaluate this result, values for St_D, M_a, and ϕ are required. Using values relevant to the experimental basis for this discussion ($St_D = 0.2$, $M_a = 1$, $\phi = 30°$), Table 3 is computed for several azimuthal extents ($\delta\theta$). In addition to the acoustic power (W_p), Table 3 also contains the energy of the Gaussian (E) and the acoustic power normalized by the Gaussian energy. Since the Gaussian always has unit amplitude, its energy changes as the extent ($\delta\theta$) changes. It is therefore possible that the acoustic power could be simply scaling with the energy of the Gaussian. Normalizing the acoustic power by the Gaussian energy scales eliminates this variable.

$\delta\theta$	β	$E = C_n C_n$	W_p	W_p/E
0.01	0.038	7.53×10^{-3}	2.24×10^{-3}	0.297
0.1	0.377	7.53×10^{-2}	0.223	2.97
0.2	0.755	0.151	0.892	5.93
0.5	1.89	0.376	5.22	13.9
1.0	3.77	0.681	12.4	18.2
10	37.7	0.995	18.7	18.8

Table 3: Radiated power versus azimuthal extent ($\delta\theta$) for $St_D = 0.2$, $M_a = 1$, & $\phi = 30°$.

The first thing to notice is that the normalized power increases with increasing $\delta\theta$. This shows that the radiating efficiency of a source increases with increasing azimuthal extent. As $\delta\theta \to \infty$ (i.e. the extent limits to an axisymmetric source), the acoustic power saturates indicating that sources which are approximately axisymmetric can be treated as axisymmetric when considering their radiation behavior.

While not tabulated, there are additional behaviors of note with regard to varying the Strouhal number. For $\delta\theta \ll 1$, the acoustic power is independent of the Strouhal number. When $\delta\theta \geq 1$, only the zeroth order Fourier coefficient is significantly non-zero so the acoustic power behaves like a zeroth order Bessel function (i.e. J_0) when varying the Strouhal number. Obviously, the complete far-field pressure (10) has many dependencies resulting in a complex behavior that cannot be easily described in words—and this is a very simplistic model. The preceding highlights a few of the relevant parameters for the purpose of the present discussion.

The result of this azimuthal extent model provides a basis for some of the suppositions made in the model description (§6.1) and at the end of §4.3. Exciting the jet with higher order azimuthal modes restricts the azimuthal extent of the structures, which should create a corresponding restriction of the sources. Within the scope of this model, this result shows that these confined sources are less efficient radiators. If one imagines exciting azimuthal mode three as three independent sources each with an extent of $\delta\theta = 0.1$, the combined power would be $3 \times 2.97 = 8.91$ (where 2.97 came from the appropriate entry in Table 3). Thus, several azimuthally smaller sources are still weaker radiators than one axisymmetric source. As an alternative example, the acoustic power for a purely axisymmetric source using the same parameters as those used to generate Table 3 ($St_D = 0.2$, $M_a = 1$, $\phi = 30°$) is $W_p = 18.8$ while the acoustic power for a purely mode three source with the same parameters is $W_p = 8.14 \times 10^{-6}$. The disparity in this case is very much larger because of the use of a single simple harmonic as the model of the azimuthal extent. In reality, the decrease in radiating efficiency created by exciting mode three is probably somewhere between the two examples just discussed since a simple harmonic is an over-simplification and the neighboring structures in an $m = 3$ excited jet aren't actually independent.

If the azimuthal extent of a structure were to vary over the lifetime of a structure (as should be expected given the highly turbulent nature of the jet), the above provides a possible model for the inductive argument made at the end of §4.3. While it is possible to numerically model a source with time dependent Fourier coefficients, it is analytically intractable and the model already presented provides a sufficient basis for a discussion. When a structure is first created (i.e. has small azimuthal extent), this model indicates that it is a relatively inefficient radiator. Under the right circumstances (see §6.1) this structure will experience a period of time during which it has a large azimuthal extent and high noise source energy that would result in a period of increased radiating efficiency and radiating power. This period of increased radiation would be a noise event. This uncouples the axial frequency (which should be directly related to the intermittence) from the event width (which the data show is a fraction of the intermittence) while still maintaining a close relationship between the two quantities through the governing dynamics of vortex evolution.

6.3 Noise Event Point of Origin

It is tempting to think of the oscillations of the wave-packet models as being synonymous with the large-scale structures. While they are obviously related, linking them so strongly is not warranted. The shape and placement of the envelope function plays an important role in this interpretation. For the sake of a discussion, it is assumed that the oscillating factor and the envelope are tuned to mimic the growth and decay characteristics of the large-scale structures. If linked in this way, the conclusion is as follows. Once a structure has enough energy to be dynamically relevant, it radiates continually as it propagates downstream until it is destroyed by viscous forces. Given that the structures in the jet can be of significant size for several jet diameters preceding the end of the potential core (§2.2), this would imply that the noise source is highly distributed (i.e. highly non-compact). It is worth noting that this kind of radiation behavior has been known for many years to exist in a different jet noise generation mechanism, Mach wave radiation [78]. In these flows, supersonically convecting structures produce this kind of highly non-compact noise source. This noise source has been studied at GDTL and schlieren images clearly showing the link between the structures and the Mach wave radiation are found in Kearney-Fischer *et al.* [69]. For further discussion of this noise generation mechanism, the reader should refer to the cited GDTL publication.

While it is possible that the preceding interpretation is correct, there is some evidence that may contradict that interpretation. As discussed in §2.3, previous work at GDTL has shown that these noise events have an apparent origin in a region (about five jet diameters axially) around the end of the potential core [54, 55]. This was determined through the use of a beam-forming array utilizing cross-correlation between several microphones and linear acoustic propagation to determine an event origin in space-time. If these events are generated only near the end of the potential core, then the oscillations in a wave-packet model cannot be synonymous with the large-scale

structures. At a minimum, the envelope function must describe some significant change in the flow-field that makes the structures radiation capable.

One potential problem with the determination of the space-time origin performed by Kastner *et al.* [55] and Hileman *et al.* [54] is that they used a very simple model and did not incorporate the directional dependency of the noise event characteristics (see [6] and §4.2.3). These directional characteristics can create errors in the calculation of the space-time origin. Additionally, if the noise sources do behave according to the highly non-compact model, they would likely have an apparent origin near the end of the potential core. The apparent location would arise because the shape of the outgoing wave created by the convecting source would be more elliptical rather than spherical. In calculating the origin of noise events, Kastner *et al.* and Hileman *et al*. used a fairly simple triangulation procedure that does not account for refraction effects let alone a convecting source. This does not make their work invalid (in fact their work was shown to closely match much more complex beam forming techniques); it just means that there is additional complexity buried in their results that has not been taken into account.

7 SUMMARY AND CONCLUSIONS

An experimental database from the Ohio State University Gas Dynamics and Turbulence Laboratory (GDTL) of far-field acoustic data from an excited subsonic (M_j = 0.9) jet at various temperatures (TTR = 1.0-2.5) was analyzed using the same process described in [6] (a previous work on unexcited subsonic jets based on data from NASA's Aeroacoustic Propulsion Laboratory) to determine what other characteristics of these noise events and their production could be identified. The jet was excited using an array of eight Localized Arc Filament Plasma Actuators (LAFPAs) spaced azimuthally around the nozzle exit. The excitation azimuthal modes and Strouhal number examined were m = 0, 1, & 3 and St_{DF} = 0.09-3.0, respectively. The basic characteristics of the signal analysis from this database matched those from the unexcited database [6]; indicating that the dynamics being examined are general and not facility dependent. In addition to the experimental acoustic database, conclusions and observations from previous works using LAFPAs were leveraged to inform discussion of the statistical results and their relationship to the flow-field dynamics.

The results from the excited jet exposed several important characteristics that wouldn't have been discovered without the use of excitation. Analysis of the noise events revealed the existence of a resonance condition in the jet. When the jet is excited at a frequency matching the mean intermittence of the unexcited jet, large noise amplification can occur. This phenomenon is particularly pronounced when exciting the axisymmetric mode. When this occurs, every large-scale structure is producing a noise event. Conversely, noise reduction occurs when only a fraction of the large-scale structures produce noise events. This occurred most substantially when the jet was excited with m = 3 and frequencies in the range St_{DF} = 0.5-1.0 depending on jet temperature. The other modes also produce noise reduction, but m = 3 (the highest simple azimuthal mode that could be excited by 8 LAFPAs) had the most pronounced effect. These results suggest a process in which noise sources are competing for flow energy and that these noise sources are closely related to the large-scale structures.

A preliminary experiment to explore the behavior and interaction of large-scale structures was conducted. This experiment used a 2.54 cm diameter unheated jet operated at M_j = 0.9 excited with the axisymmetric mode. The signature of the jet structures was measured by microphones placed in the near-field hydrodynamic region. By exciting the jet with very low frequencies, the impulse response of the jet was determined. The frequency range of constructive and destructive interaction between large-scale structures was determined. It was found that the peak in the energy density of the large-scale structures corresponds to the resonance condition found in the acoustic results.

Leveraging the known dynamics of the excited jet flow-field, it was possible to leverage the current results to improve the understanding of noise production. Based on the known flow-field dynamics and the acoustic results from the excited jet, a hypothetical model of the competition process was described. A brief synopsis of the model is as follows. Depending on the axial and azimuthal proximity of adjacent structures, initially separate structures can combine, work collaboratively to extract energy from the flow, or stifle each other's ability to extract energy. When the structures are able to consistently extract large amounts of flow energy, they produce strong noise events. When energy extraction is inhibited, noise production is reduced. Noise reduction through excitation is achieved by exciting the jet into a configuration that has reduced noise production while also inhibiting the naturally occurring structures.

Using a wave-packet model on a cylindrical surface, the impact of the azimuthal extent of a source was examined. By modeling the azimuthal extent as a Gaussian, it was possible to write down an analytical expression

for the far-field acoustic power. Using this expression it was shown that an axisymmetric structure is the most efficient radiator of sound (within the scope of the model). A structure covering only a fraction of the azimuth was less efficient and the efficiency increases monotonically with increasing azimuthal extent. It was proposed that a time varying azimuthal extent could explain the noise events by letting the lifetime of an event (i.e. the event width) be dictated by the time during which a structure has large azimuthal extent while the time between events (i.e. the intermittence) is dictated by the time between the large-scale structure occurrences.

The results presented in this work reveal a wealth of new information on jet noise that can be accessed by the combined techniques of exciting the jet to control the dynamics of the turbulent structures and analyzing the noise production in terms of discrete events. While the present work is far from a silver bullet solution to the problem of jet noise, it shows that there is plenty of relevant information waiting to be accessed using tools like these.

ACKNOWLEDGEMENTS

The support of this work by the Air Force of Office of Scientific Research (with Dr. John Schmisseur) and the NASA Glenn Research Center (with Drs. James Bridges and Clifford Brown) is greatly appreciated.

REFERENCES

[1] Lighthill, M.J., "On Sound Generated Aerodynamically. I. General Theory", *Proc. Roy. Soc. London Ser. A* Vol. 211, No. 1107, 1952, pp. 564-587.

[2] Jordan, P., and Gervais, Y., "Subsonic jet aeroacoustics: associating experiment, modelling and simulation", *Exp. Fluids* Vol. 44, 2008, pp. 1-21.

[3] Tam, C.K.W., Golebiowski, M., and Seiner, J.M., "On the Two Components of Turbulent Mixing Noise from Supersonic Jets", AIAA Paper 1996-1716, 1996.

[4] Viswanathan, K., "Scaling Laws and a Method for Identifying Components of Jet Noise", *AIAA J.* Vol. 44, No. 10, 2006, pp. 2274-2285.

[5] Cabana, M., Fortuné, V., and Jordan, P., "Identifying the radiating core of Lighthill's source term", *Theor. & Comput. Fluid Dyn.*, 2007, pp. 20.

[6] Kearney-Fischer, M., Sinha, A., and Samimy, M., "Time-Domain Analysis of Subsonic Jet Noise ", AIAA Paper 2012-1167, 2012.

[7] Kambe, T., and Minota, T., "Acoustic Wave Radiated by Head-On Collision of Two Vortex Rings", *Proc. Roy. Soc. London Ser. A* Vol. 386, 1983, pp. 277-308.

[8] Minota, T., and Kambe, T., "Observation of Acoustic Emission from Head-On Collision of Two Vortex Rings", *J. Sound & Vib.* Vol. 111, No. 1, 1986, pp. 51-59.

[9] Kambe, T., "Vortex sound with special reference to vortex rings: theory, computer simulations, and experiments", *Int. J. Aeroacoustics* Vol. 9, No. 1 & 2, 2010, pp. 51-89.

[10] Powell, A., "Theory of Vortex Sound", *Journal of the Acoustical Society of America* Vol. 36, No. 1, 1964, pp. 177-195.

[11] Möhring, W., "On vortex sound at low Mach number", *J. Fluid Mech.* Vol. 85, No. 4, 1978, pp. 685-691.

[12] Schram, C., Hirschbert, A., and Verzicco, R., "Sound Produced by Vortex Pairing: Prediction Based on Particle Image Velocimetry", *AIAA J.* Vol. 42, No. 11, 2004, pp. 2234-2244.

[13] Schram, C., Taubitz, S., Anthoine, J., and Hirschberg, A., "Theoretical/empirical prediction and measurement of the sound produced by vortex pairing in a low Mach number jet", *J. Sound & Vib.* Vol. 281, No. 1-2, 2005, pp. 171-187.
[14] Ran, H., and Colonius, T., "Numerical Simulation of the Sound Radiated from a Turbulent Vortex Ring", *Int. J. Aeroacoustics* Vol. 8, No. 4, 2009, pp. 317-336.
[15] Ko, N.W.M., Leung, R.C.K., and Tang, C.C.K., "The interaction of perturbed vortex rings and its sound generation. Part II", *J. Sound & Vib.* Vol. 228, No. 3, 1999, pp. 511-541.
[16] Fedorchenko, A.T., "On some fundamental flaws in present aeroacoustic theory", *J. Sound & Vib.* Vol. 232, No. 4, 2000, pp. 719-782.
[17] Tang, S.K., and Ko, N.W.M., "Sound sources in the interactions of two inviscid two-dimensional vortex pairs", *J. Fluid Mech.* Vol. 419, 2000, pp. 177-201.
[18] Samimy, M., Zaman, K.B.M.Q., and Reeder, M.F., "Effect of Tabs on the Flow and Noise Field of an Axisymmetric Jet", *AIAA J.* Vol. 31, No. 4, 1993, pp. 609-619.
[19] Zaman, K.B.M.Q., Reeder, M.F., and Samimy, M., "Control of an Axisymmetric Jet Using Vortex Generators", *Phys. Fluids* Vol. 6, No. 2, 1994, pp. 778-793.
[20] Kim, J., and Samimy, M., "Mixing Enhancement via Nozzle Trailing Edge Modifications in a High Speed Rectangular Jet", *Phys. Fluids* Vol. 11, No. 9, 1999, pp. 2731-2742.
[21] Saiyed, N.H., Mikkelsen, K.L., and Bridges, J.E., "Acoustics and Thrust of Quiet Separate-Flow High-Bypass-Ratio Nozzles", *AIAA J.* Vol. 41, No. 3, 2003, pp. 372-378.
[22] Callender, B., Gutmark, E., and Martens, S., "Far-Field Acoustic Investigation into Chevron Nozzle Mechanisms and Trends", *AIAA J.* Vol. 43, No. 1, 2004, pp. 87-95.
[23] Viswanathan, K., "Nozzle Shaping for Reduction of Jet Noise from Single Jets", *AIAA J.* Vol. 43, No. 5, 2005, pp. 1008-1022.
[24] Crow, S.C., and Champagne, F.H., "Orderly Structure in Jet Turbulences", *J. Fluid Mech.* Vol. 48, No. 3, 1971, pp. 547-591.
[25] Kibens, V., "Discrete Noise Spectrum Generated by an Acoustically Excited Jet", *AIAA J.* Vol. 18, No. 4, 1980, pp. 434-441.
[26] Zaman, K.B.M.Q., and Hussain, A.K.M.F., "Vortex pairing in a circular jet under controlled excitation. Part 1. General jet response", *J. Fluid Mech.* Vol. 101, No. 3, 1980, pp. 449-491.
[27] Zaman, K.B.M.Q., and Hussain, A.K.M.F., "Turbulence Suppression in Free Shear Flows by Controlled Excitation", *J. Fluid Mech.* Vol. 103, 1981, pp. 133-159.
[28] Gutmark, E., and Ho, C.M., "Preferred Modes and the Spreading Rated of Jets", *Phys. Fluids* Vol. 26, No. 10, 1983, pp. 2932-2938.
[29] Ho, C.M., and Huerre, P., "Perturbed free shear layers", *Ann. Rev. Fluid Mech.* Vol. 16, 1984, pp. 365-424.
[30] Cohen, J., and Wygnanski, I., "The evolution of instabilities in the axisymmetric jet. Part 1 the linear growth of disturbances near nozzle", *J. Fluid Mech.* Vol. 176, 1987, pp. 191-219.
[31] Monkewitz, P., Bechert, D., Barsikow, B., and Lehmann, B., "Self-excited oscillations and mixing in a heated round jet", *J. Fluid Mech.* Vol. 213, 1990, pp. 611-639.
[32] Lesshafft, L., Huerre, P., and Sagaut, P., "Aerodynamic Sound Generation by Global Modes in Hot Jets", *J. Fluid Mech.* Vol. 647, 2010, pp. 473-489.
[33] Jendoubi, S., and Strykowski, P.J., "Absolute and Convective Instability of Axisymmetric Jets with External Flow", *Phys. Fluids* Vol. 6, No. 9, 1994, pp. 3000-3009.

[34] Michalke, A., "Survey on Jet Instability Theory", *Prog. Aerosp. Sci.* Vol. 21, 1984, pp. 159-199.
[35] Jubelin, B., "New Experimental Studies on Jet Noise Amplification", AIAA Paper 1980-0961, 1980.
[36] Lu, H.Y., "Effect of Excitation on Coaxial Jet Noise", *AIAA J.* Vol. 21, No. 2, 1983, pp. 214-220.
[37] Ahuja, K.K., and Blakney, D.F., "Tone Excited Jets. IV - Acoustic Measurements", *J. Sound & Vib.* Vol. 102, No. 1, 1985, pp. 93-117.
[38] Ahuja, K.K., and Whiffen, M.C., "Tone Excited Jets. II - Flow Visualization", *J. Sound & Vib.* Vol. 102, No. 1, 1985, pp. 63-69.
[39] Lepicovsky, J., Ahuja, K.K., and Burrin, R.H., "Tone Excited Jets. III - Flow Measurements", *J. Sound & Vib.* Vol. 102, No. 1, 1985, pp. 71-91.
[40] Lepicovsky, J., Ahuja, K.K., Brown, W.H., and Burrin, R.H., "Coherent Large-Scale Structures in High Reynolds Number Supersonic Jets", NASA CR 3952, 1985.
[41] Troutt, T.R., and McLaughlin, D.K., "Experiments on the flow and acoustic properties of a moderate-Reynolds-number supersonic jet", *J. Fluid Mech.* Vol. 116, 1982, pp. 123-156.
[42] Morrison, G.L., "Effects of Artificial Excitation Upon a Low Reynolds Number Mach 2.5 Jet", *AIAA Technical Notes* Vol. 21, No. 6, 1983, pp. 920-923.
[43] Samimy, M., Kim, J.H., Kastner, J., Adamovich, I., and Utkin, Y., "Active Control of a Mach 0.9 Jet for Noise Mitigation Using Plasma Actuators", *AIAA J.* Vol. 45, No. 4, 2007, pp. 890-901.
[44] Samimy, M., Kim, J.-H., Kastner, J., Adamovich, I., and Utkin, Y., "Active control of high-speed and high-Reynolds-number jets using plasma actuators", *J. Fluid Mech.* Vol. 578, 2007, pp. 305-330.
[45] Samimy, M., Kim, J.-H., Kearney-Fischer, M., and Sinha, A., "Acoustic and Flow Fields of an Excited High Reynolds Number Axisymmetric Supersonic Jet", *J. Fluid Mech.* Vol. 656, 2010, pp. 507-529.
[46] Samimy, M., Kearney-Fischer, M., Kim, J.-H., and Sinha, A., "High-Speed and High-Reynolds-Number Jet Control Using Localized Arc Filament Plasma Actuators", *J. Propuls. & Power* Vol. 28, No. 2, 2012, pp. 269-280.
[47] Samimy, M., Adamovich, I., Webb, B., Kastner, J., Hileman, J., Keshav, S., and Palm, P., "Development and characterization of plasma actuators for high-speed jet control", *Exp. Fluids* Vol. 37, No. 4, 2004, pp. 577-588.
[48] Kim, J.-H., Nishihara, M., Adamovich, I.V., Samimy, M., Gorbatov, S.V., and Pliavaka, F.V., "Development of Localized Arc Filament RF Plasma Actuators for High-Speed and High Reynolds Number Flow Control", *Exp. Fluids* Vol. 49, No. 2, 2010, pp. 497–511.
[49] Kim, J.-H., Kastner, J., and Samimy, M., "Active Control of a High Reynolds Number Mach 0.9 Axisymmetric Jet", *AIAA J.* Vol. 47, No. 1, 2009, pp. 116-128.
[50] Kearney-Fischer, M., and Samimy, M., "Noise Control of a High Reynolds Number Mach 1.3 Heated Jet Using Plasma Actuators", AIAA Paper 2010-0013, 2010.
[51] Kearney-Fischer, M., Kim, J.-H., and Samimy, M., "Flow Control of a High Reynolds Number Mach 1.3 Heated Jet Using Plasma Actuators", AIAA Paper 2010-4418, 2010.
[52] Kearney-Fischer, M., Kim, J.-H., and Samimy, M., "Noise Control of a High Reynolds Number High Speed Heated Jet Using Plasma Actuators", *Int. J. Aeroacoustics* Vol. 10, No. 5-6, 2011, pp. 635 – 658.

[53] Kearney-Fischer, M., Kim, J.-H., and Samimy, M., "Control of a high Reynolds number Mach 0.9 heated jet using plasma actuators", *Phys. Fluids* Vol. 21, 2009, pp. 095101.
[54] Hileman, J., Thurow, B., Caraballo, E., and Samimy, M., "Large-scale structure evolution and sound emission in high-speed jets: real-time visualization with simultaneous acoustic measurements", *J. Fluid Mech.* Vol. 544, 2005, pp. 277–307.
[55] Kastner, J., Kim, J.-H., and Samimy, M., "A study of the correlation of large-scale structure dynamics and far-field radiated noise in an excited Mach 0.9 jet", *Int. J. Aeroacoustics* Vol. 8, No. 3, 2009, pp. 231–259.
[56] Grassucci, D., Camussi, R., Kerhervé, F., Jordan, P., and Grizzi, S., "Using Wavelet transforms and Linear Stochastic Estimation to study nearfield and turbulent velocity signatures in free jets", AIAA Paper 2010-3954, 2010.
[57] Cavalieri, A.V.G., Jordan, P., Gervais, Y., Wei, M., and Freund, J.B., "Intermittent sound generation and its control in a free-shear flow", *Phys. Fluids* Vol. 22, 2010, pp. 115113.
[58] Cavalieri, A.V.G., Jordan, P., Agarwal, A., and Gervais, Y., "Jittering wave-packet models for subsonic jet noise", *J. Sound & Vib.* Vol. 330, 2011, pp. 4474–4492.
[59] Kœnig, M., Cavalieri, A., Jordan, P., Delville, J., Gervais, Y., Papamoschou, D., Samimy, M., and Lele, S., "Farfield filtering and source imaging for the study of jet noise", AIAA Paper 2010-3779, 2010.
[60] Guj, G., Carley, M., Camussi, R., and Ragni, A., "Acoustic identification of coherent structures in a turbulent jet", *J. Sound & Vib.* Vol. 259, No. 5, 2003, pp. 1037-1065.
[61] Juve, D., Sunyach, M., and Comte-Bellot, G., "Intermittency of the Noise Emission in Subsonic Cold Jets", *J. Sound & Vib.* Vol. 71, No. 3, 1980, pp. 319-332.
[62] Low, K.R., Berger, Z.P., Lewalle, J., El-Hadidi, B., and Glauser, M.N., "Correlations and Wavelet Based Analysis of Near-Field and Far-Field Pressure of a Controlled High Speed Jet", AIAA Paper 2011-4020, 2011.
[63] Wei, M., and Freund, J.B., "A noise-controlled free shear flow", *J. Fluid Mech.* Vol. 546, 2005, pp. 123-152.
[64] Kastner, J., Samimy, M., Hileman, J., and Freund, J.B., "Comparison of Noise Mechanisms in High and Low Reynolds Number High-Speed Jets", *AIAA J.* Vol. 44, No. 10, 2006, pp. 2251-2258.
[65] Kœnig, M., Cavalieri, A.V.G., Jordan, P., Delville, J., Gervais, Y., and Papamoschou, D., "Farfield filtering of subsonic jet noise: Mach and Temperature effects", AIAA Paper 2011-2926, 2011.
[66] Kœnig, M., Cavalieri, A.V.G., Jordan, P., and Gervais, Y., "Intermittency of the azimuthal components of the sound radiated by subsonic jets", AIAA Paper 2011-2746, 2011.
[67] Tanna, H.K., "An Experimental Study of Jet Noise. Part I. Turbulent Mixing Noise", *J. Sound & Vib.* Vol. 50, No. 3, 1977, pp. 405-428.
[68] Kerechanin II, C.W., Samimy, M., and Kim, J.H., "Effects of Nozzle Trailing Edges on Acoustic Field of Supersonic Rectangular Jet", *AIAA J.* Vol. 39, No. 6, 2001, pp. 1065-1070.
[69] Kearney-Fischer, M., Kim, J.-H., and Samimy, M., "A Study of Mach Wave Radiation Using Active Control", *J. Fluid Mech.* Vol. 681, 2011, pp. 261-292.
[70] Suzuki, T., and Colonius, T., "Instability waves in a subsonic round jet detected using a near-field phased microphone array", *J. Fluid Mech.* Vol. 565, 2006, pp. 197-226.

[71] Hall, A.M., and Glauser, M.N., "An experimental analysis of the modal characteristics intrinsic to both the heated and cold jet", AIAA Paper 2009-1238, 2009.
[72] Kastner, J., "Far-Field Radiated Noise Mechanisms in High Reynolds Number and High-Speed Jets", *Mechanical Engineering*: Ohio State University, 2007.
[73] Crighton, D.G., and Huerre, P., "Shear-layer pressure fluctuations and superdirective acoustic sources", *J. Fluid Mech.* Vol. 220, 1990, pp. 355-368.
[74] Hall, J.W., Pinier, J., Hall, A., and Glauser, M., "Two-point correlations of the near and far-field pressure in a transonic jet", ASME Paper FEDSM2006-98458, 2006.
[75] Sinha, A., Kearney-Fischer, M., Alkandry, H., and Samimy, M., "The Impulse Response of a High-Speed Jet Forced with Localized Arc Filament Plasma Actuators ", AIAA Paper 2012-0000, 2012.
[76] Utkin, Y.G., Keshav, S., Kim, J.-H., Kastner, J., Adamovich, I.V., and Samimy, M., "Development and Use of Localized Arc Filament Plasma Actuators for High-Speed Flow Control", *J. Phys. D: Appl. Phys.* Vol. 40, No. 3, 2007, pp. 685-694.
[77] Kim, J.-H., and Samimy, M., "Effects of Active Control on the Flow Structure in a High Reynolds Number Supersonic Jet", *International Journal of Flow Control* Vol. 1, No. 2, 2009, pp. 99-117.
[78] Tam, C.K.W., "Directional acoustic radiation from a supersonic jet generated by shear layer instability", *J. Fluid Mech.* Vol. 46, No. 4, 1971, pp. 757-768.